LOAN DOCUMENT

PHOTOGRAPH THIS SHEET

DTIC ACCESSION NUMBER

LEVEL

INVENTORY

EPA-600/R-98-029

DOCUMENT IDENTIFICATION

MAR 98

DISTRIBUTION STATEMENT A
Approved for Public Release
Distribution Unlimited

DISTRIBUTION STATEMENT

ACCESSION FOR
NTIS GRA&I
DTIC TRAC
UNANNOUNCED
JUSTIFICATION

BY
DISTRIBUTION/
AVAILABILITY CODES

DISTRIBUTION	AVAILABILITY AND/OR SPECIAL	
A-1		

DISTRIBUTION STAMP

DATE ACCESSIONED

DATE RETURNED

19990609 033

DATE RECEIVED IN DTIC

REGISTERED OR CERTIFIED NUMBER

PHOTOGRAPH THIS SHEET AND RETURN TO DTIC-FDAC

HANDLE WITH CARE

DTIC FORM 70A JUN 90 — DOCUMENT PROCESSING SHEET — PREVIOUS EDITIONS MAY BE USED UNTIL STOCK IS EXHAUSTED.

LOAN DOCUMENT

PP 309

United States
Environmental Protection
Agency

EPA-600/R-98-029

March 1998

EPA

Research and Development

HEAT TRANSFER EVALUATION
OF HFC-236fa IN CONDENSATION
AND EVAPORATION

Prepared for

Strategic Environmental Research and
Development Program

Prepared by

National Risk Management
Research Laboratory
Research Triangle Park, NC 27711

FOREWORD

The U.S. Environmental Protection Agency is charged by Congress with protecting the Nation's land, air, and water resources. Under a mandate of national environmental laws, the Agency strives to formulate and implement actions leading to a compatible balance between human activities and the ability of natural systems to support and nurture life. To meet this mandate, EPA's research program is providing data and technical support for solving environmental problems today and building a science knowledge base necessary to manage our ecological resources wisely, understand how pollutants affect our health, and prevent or reduce environmental risks in the future.

The National Risk Management Research Laboratory is the Agency's center for investigation of technological and management approaches for reducing risks from threats to human health and the environment. The focus of the Laboratory's research program is on methods for the prevention and control of pollution to air, land, water, and subsurface resources; protection of water quality in public water systems; remediation of contaminated sites and groundwater; and prevention and control of indoor air pollution. The goal of this research effort is to catalyze development and implementation of innovative, cost-effective environmental technologies; develop scientific and engineering information needed by EPA to support regulatory and policy decisions; and provide technical support and information transfer to ensure effective implementation of environmental regulations and strategies.

This publication has been produced as part of the Laboratory's strategic long-term research plan. It is published and made available by EPA's Office of Research and Development to assist the user community and to link researchers with their clients.

E. Timothy Oppelt, Director
National Risk Management Research Laboratory

EPA REVIEW NOTICE

EPA-600/R-98-029
March 1998

HEAT TRANSFER EVALUATION OF HFC-236fa IN CONDENSATION AND EVAPORATION

by

S.-M. Tzuoo
M.B. Pate
Iowa State University
Ames, IA 50011

EPA Purchase Order No. 5D2520NAEX

Project Officer:

Theodore G. Brna
U.S. Environmental Protection Agency
National Risk Management Research Laboratory
Air Pollution Prevention and Control Division
Research Triangle Park, NC 27711

Prepared for:

U.S. ENVIRONMENTAL PROTECTION AGENCY
OFFICE OF RESEARCH AND DEVELOPMENT
WASHINGTON, DC 20460

ABSTRACT

The shell-side heat transfer performance of hydrofluorocarbon (HFC)-236fa, which is considered as a potential substitute for replacing chlorofluorocarbon (CFC)-114 in Navy shipboard chillers, was evaluated in this study for both conventional finned tubes (1024-fpm and 1575-fpm tubes) and high performance enhanced (Turbo-CII, Turbo-B, and Turbo-BII) tubes.

Condensation of oil-free HFC-236fa was conducted on a 1024-fpm, a 1575-fpm, and a Turbo-CII tube. Pool boiling on four tube types (1024-fpm, 1575-fpm, Turbo-B, and Turbo-BII) was tested not only for pure HFC-236fa but also for HFC-236fa mixed with 1% and 3% lubricant by weight. The polyol ester lubricant used has a viscosity of 340 SSU at 37.8°C (100°F) and the trade name of Castrol Icematic SW-68. The above tubes which have nominal outside diameters of 19.1 mm (3/4 in.) were evaluated at a saturation temperature of 40°C for condensation and 2°C for pool boiling over the heat flux range of 15 kW/m^2 to 40 kW/m^2.

Heat transfer was improved for HFC-236fa by using the high performance enhanced tubes. Specifically, the Turbo-CII tube performed better than the two conventional finned tubes in the condensation testing, while the performance of the Turbo-B and Turbo-BII tubes was superior to the two conventional finned tubes in the pool boiling testing.

The maximum increase in heat transfer coefficients for the Turbo-CII tube was 80% relative to the 1024-fpm tube and 70% relative to the 1575-fpm tube, while for the Turbo-B tube, it was 0.7 and 1.2 times greater than for the 1024-fpm tube and 1575-fpm tube, respectively. In addition, the Turbo-BII tube gave boiling heat transfer coefficients up to 80% larger than those of the Turbo-B tube.

The heat transfer performance of HFC-236fa was compared with the CFC-114 and HFC-236ea data obtained in earlier studies using the same test facility. For all tube types tested except the Turbo-CII tube, the heat transfer results showed that HFC-236fa performed better than CFC-114 and HFC-236ea during both shell-side condensation and pool boiling. The heat transfer coefficients for HFC-236fa during condensation were up to 40% larger than those for CFC-114 and up to 30% larger than those for HFC-236ea, while the pool boiling coefficients were up to 80% higher for HFC-236fa compared with CFC-114 and up to 70% higher compared with HFC-236ea. The condensation heat transfer coefficients for the Turbo-CII tube were similar for both HFC-236fa and HFC-236ea; the deviation was within 10%.

The effects of compressor oil on heat transfer performance during pool boiling were investigated. The presence of up to 3% oil (by weight) in HFC-236fa affected the boiling performance by less than a 10% deviation from the pure HFC-236fa results for all but one of the tubes tested. The Turbo-BII tube, the only exception,

showed an increase in boiling coefficients of up to 30% over the pure refrigerant values for the testing with 1% oil and up to 15% with 3% oil.

This report was submitted in fulfillment of EPA Purchase Order Number 5D2520NAEX by Iowa State University under the sponsorship of the U.S. Environmental Protection Agency with funding from the EPA/DoD/DOE Strategic Environmental Research and Development Program* (SERDP). This report covers the period from September 1995 to May 1996.

---

* A joint program of the Department of Defense, the Department of Energy, and the Environmental Protection Agency.

CONTENTS

Abstract ii

List of Figures vi

List of Tables viii

List of Abbreviations and Symbols xi

Acknowledgments xiii

Chapter 1. Introduction 1

Background 1

Research program 2

Chapter 2. Conclusions 4

Chapter 3. Recommendations 6

Chapter 4. Experimental Description 7

Experimental apparatus 7

Instrumentation and calibration 10

Experimental procedures 11

Data reduction 12

Experimental uncertainty of data 14

Chapter 5. Condensation Results 16

Overview 16

Condensation results for HFC-236fa 17

Comparison with an existing correlation 17

Comparison of results for CFC-114, HFC-236ea, and HFC-236fa 23

Summary 23

Chapter 6. Pool Boiling Results 27

Overview 27

Pool boiling results for HFC-236fa 28

Comparison of results for CFC-114, HFC-236ea, and HFC-236fa 31

Pool boiling results for HFC-236fa/oil mixtures 31

Summary 43

References 46

Contents (continued)

Appendix A. Refrigerant Properties 48
Appendix B. Geometric Specifications of Tubes 49
Appendix C. Tabulated Data 50
Appendix D. Derivation of Uncertainty Analysis Equations 66

LIST OF FIGURES

Number		Page
4.1	Schematic of test facility for condensation tests	8
4.2	Schematic of test facility for pool boiling tests	9
5.1	Condensation heat transfer coefficients for HFC-236fa using the Turbo-CII, 1024-fpm, and 1575-fpm tubes at T_{sat} = 40°C	18
5.2	Temperature difference effects on condensation heat transfer coefficients for HFC-236fa at T_{sat} = 40°C	19
5.3	Correlation comparison of HFC-236fa for the 1024-fpm and 1575-fpm tubes (tube dia. = 19.1 mm) at T_{sat} = 40°C	21
5.4	Correlation comparison of HFC-236fa for the Turbo-CII tube (tube dia. = 19.1 mm) at T_{sat} = 40°C	22
5.5	Condensation heat transfer coefficients for HFC-236fa, HFC-236ea, and CFC-114 using the 1024-fpm tube at T_{sat} = 40°C	24
5.6	Condensation heat transfer coefficients for HFC-236fa, HFC-236ea, and CFC-114 using the 1575-fpm tube at T_{sat} = 40°C	25
5.7	Condensation heat transfer coefficients for HFC-236fa and HFC-236ea using the Turbo-CII tube at T_{sat} = 40°C	26
6.1	Heat transfer coefficients for HFC-236fa using the Turbo-BII, Turbo-B, 1024-fpm, and 1575-fpm tubes in pool boiling at T_{sat} = 2°C	29
6.2	Excess temperature effects on heat transfer coefficients for HFC-236fa in pool boiling at T_{sat} = 2°C	30
6.3	Heat transfer coefficients for HFC-236fa, HFC-236ea, and CFC-114 using the 1024-fpm tube in pool boiling at T_{sat} = 2°C	32
6.4	Heat transfer coefficients for HFC-236fa, HFC-236ea, and CFC-114 using the 1575-fpm tube in pool boiling at T_{sat} = 2°C	33
6.5	Heat transfer coefficients for HFC-236fa and HFC-236ea using the Turbo-B tube in pool boiling at T_{sat} = 2°C	34
6.6	Heat transfer coefficients for HFC-236fa and HFC-236ea using the Turbo-BII tube in pool boiling at T_{sat} = 2°C	35

List of Figures (continued)

6.7 Oil effects on heat transfer coefficients of HFC-236fa using the 1024-fpm tube in pool boiling at T_{sat} = 2°C 36

6.8 Oil effects on heat transfer coefficients of HFC-236fa using the 1575-fpm tube in pool boiling at T_{sat} = 2°C 37

6.9 Oil effects on heat transfer coefficients of HFC-236fa using the Turbo-B tube in pool boiling at T_{sat} = 2°C 38

6.10 Oil effects on heat transfer coefficients of HFC-236fa using the Turbo-BII tube in pool boiling at T_{sat} = 2°C 39

6.11 Comparison of the Turbo-BII, Turbo-B, 1024-fpm, and 1575-fpm tubes in pool boiling of HFC-236fa with 1% oil at T_{sat} = 2°C 44

6.12 Comparison of the Turbo-BII, Turbo-B, 1024-fpm, and 1575-fpm tubes in pool boiling of HFC-236fa with 3% oil at T_{sat} = 2°C 45

LIST OF TABLES

Number		Page
4.1	Uncertainty in the shell-side heat transfer coefficients for condensation	15
4.2	Uncertainty in the shell-side heat transfer coefficients for pool boiling	15
A.1	Properties of HFC-236ea	48
B.1	Geometric specifications of tubes in SI units	49
B.2	Geometric specifications of tubes in English units	49
C.1	Condensation of HFC-236fa on the 1024-fpm tube at a saturation temperature of 40°C (primary run)	51
C.2	Condensation of HFC-236fa on the 1024-fpm tube at a saturation temperature of 40°C (repeat run)	51
C.3	Condensation of HFC-236fa on the 1575-fpm tube at a saturation temperature of 40°C (primary run)	52
C.4	Condensation of HFC-236fa on the 1575-fpm tube at a saturation temperature of 40°C (repeat run)	52
C.5	Condensation of HFC-236fa on the Turbo-CII tube at a saturation temperature of 40°C (primary run)	53
C.6	Condensation of HFC-236fa on the Turbo-CII tube at a saturation temperature of 40°C (repeat run)	53
C.7	Pool boiling of HFC-236fa on the 1024-fpm tube at a saturation temperature of 2°C (primary run)	54
C.8	Pool boiling of HFC-236fa on the 1024-fpm tube at a saturation temperature of 2°C (repeat run)	54
C.9	Pool boiling of HFC-236fa on the 1575-fpm tube at a saturation temperature of 2°C (primary run)	55
C.10	Pool boiling of HFC-236fa on the 1575-fpm tube at a saturation temperature of 2°C (repeat run)	55
C.11	Pool boiling of HFC-236fa on the Turbo-B tube at a saturation temperature of 2°C (primary run)	56

List of Tables (continued)

C.12 Pool boiling of HFC-236fa on the Turbo-B tube at a saturation temperature of 2°C (repeat run) 56

C.13 Pool boiling of HFC-236fa on the Turbo-BII tube at a saturation temperature of 2°C (primary run) 57

C.14 Pool boiling of HFC-236fa on the Turbo-BII tube at a saturation temperature of 2°C (repeat run) 57

C.15 Pool boiling of HFC-236fa with 1% oil on the 1024-fpm tube at a saturation temperature of 2°C (primary run) 58

C.16 Pool boiling of HFC-236fa with 1% oil on the 1024-fpm tube at a saturation temperature of 2°C (repeat run) 58

C.17 Pool boiling of HFC-236fa with 1% oil on the 1575-fpm tube at a saturation temperature of 2°C (primary run) 59

C.18 Pool boiling of HFC-236fa with 1% oil on the 1575-fpm tube at a saturation temperature of 2°C (repeat run) 59

C.19 Pool boiling of HFC-236fa with 1% oil on the Turbo-B tube at a saturation temperature of 2°C (primary run) 60

C.20 Pool boiling of HFC-236fa with 1% oil on the Turbo-B tube at a saturation temperature of 2°C (repeat run) 60

C.21 Pool boiling of HFC-236fa with 1% oil on the Turbo-BII tube at a saturation temperature of 2°C (primary run) 61

C.22 Pool boiling of HFC-236fa with 1% oil on the Turbo-BII tube at a saturation temperature of 2°C (repeat run) 61

C.23 Pool boiling of HFC-236fa with 1% oil on the 1024-fpm tube at a saturation temperature of 2°C (primary run) 62

C.24 Pool boiling of HFC-236fa with 1% oil on the 1024-fpm tube at a saturation temperature of 2°C (repeat run) 62

C.25 Pool boiling of HFC-236fa with 1% oil on the 1575-fpm tube at a saturation temperature of 2°C (primary run) 63

C.26 Pool boiling of HFC-236fa with 1% oil on the 1575-fpm tube at a saturation temperature of 2°C (repeat run) 63

C.27 Pool boiling of HFC-236fa with 1% oil on the Turbo-B tube at a saturation temperature of 2°C (primary run) 64

List of Tables (continued)

C.28 Pool boiling of HFC-236fa with 1% oil on the Turbo-B tube at a saturation temperature of 2°C (repeat run) 64

C.29 Pool boiling of HFC-236fa with 1% oil on the Turbo-BII tube at a saturation temperature of 2°C (primary run) 65

C.30 Pool boiling of HFC-236fa with 1% oil on the Turbo-BII tube at a saturation temperature of 2°C (repeat run) 65

LIST OF ABBREVIATIONS AND SYMBOLS

ABBREVIATIONS

a	constant in the Webb and Murawski correlation
A	surface area (m^2)
Cp	specific heat at constant pressure (J/kg·K)
D	tube diameter (m)
fpi	fins per inch
fpm	fins per meter
h	shell-side heat transfer coefficient ($W/m^2 \cdot K$)
h_i	in-tube heat transfer coefficient ($W/m^2 \cdot K$)
i	enthalpy (J/kg)
k	thermal conductivity (W/m·K)
L	tube length (m)
LMTD	logarithmic mean temperature difference (°C)
$\dot{m}$	mass flow rate (kg/s)
N/A	not available
Pr	Prandtl number
q	heat transfer rate (W)
R	thermal resistance (K/W)
Re	Reynolds number
SSU	Saybolt second universal
STC	Sieder-Tate coefficient (a constant)
T	temperature (°C)
ΔT	temperature difference between the tube wall and the saturated refrigerant (°C)
U_o	overall heat transfer coefficient based on the outer surface area of a tube ($W/m^2 \cdot K$)
UN	uncertainty in heat transfer coefficient (± %)

SYMBOLS

Γ	condensate mass flow rate per unit tube length (kg/m·s)
π	a constant (= 3.14159)
μ	dynamic viscosity (N·s/m^2)

Superscripts

"	unit area basis (1/m^2)
n	exponent in the Webb and Murawski correlation

Subscripts

av	average
i	tube-side (in-tube); inside
in	inlet
liq	liquid
N	total number of tube rows measured from the top row of a bundle
NR	row number counted from the top row of a bundle
o	shell-side; outside
out	outlet
r	root
sat	saturated refrigerant
vap	vapor
w	tube wall

ACKNOWLEDGMENTS

This research was supported by the Environmental Protection Agency (EPA) under Purchase Order Number 5D2520NAEX in cooperation with the United States Navy. Funding for this work was provided by the Strategic Environmental Research and Development Program (SERDP) through the EPA (a joint program of the Department of Defense, the Department of Energy, and the Environmental Protection Agency), and this sponsor is gratefully acknowledged.

The authors would like to express their gratitude to the project officer, Theodore G. Brna, for his help and suggestions throughout the work.

Special thanks are extended to the Wolverine Tube Inc. for providing the test tubes (1024-fpm, 1575-fpm, Turbo-CII, Turbo-B, and Turbo-BII tubes), and the Trane Co. for supplying the spring-type turbulators.

The support of Department of Mechanical Engineering at Iowa State University where this work was done is also greatly appreciated.

(Intentionally Blank)

CHAPTER 1

INTRODUCTION

BACKGROUND

Shell-and-tube heat exchangers in Navy shipboard chillers presently use integral finned tubes (748-fpm and 1024-fpm tubes) and chlorofluorocarbon (CFC)-114 as the working refrigerant. A new refrigerant, hydrofluorocarbon (HFC)-236fa, does not reduce stratospheric ozone and is considered to be a potential substitute for CFC-114 which is harmful to the ozone layer. Thus, this research evaluates the heat transfer coefficients for HFC-236fa on the outside of a single horizontal tube with a nominal outside diameter of 19.1 mm (3/4 in.). HFC-236fa has a molecular formula of $CF_3CH_2CF_3$ and a molecular weight of 152.01, and its normal boiling point is −1.1°C. In addition, it is non-flammable as is CFC-114. The basic properties of HFC-236fa at the operating temperatures of 2°C and 40°C are presented in Appendix A.

The depletion of stratospheric ozone by CFCs was suspected in the 1970s, and strong evidence of this effect resulted in the international phase-out requirement of CFCs by the 1987 Montreal Protocol and its subsequent amendments. Alternative refrigerants, such as the non-toxic and non-flammable HFC-based substances, were considered to replace CFCs that have been used in refrigeration applications for decades.

Because the phase-out of CFC-114 took effect at the end of 1995 in the United States, three successive stages of investigation (Phase I, Phase II, and Phase III) were supported at Iowa State University by the EPA (Environmental Protection Agency) in cooperation with the U. S. Navy to determine the heat transfer performance of two ozone-friendly alternatives (HFC-236ea and HFC-236fa) for CFC-114. Each of these three phases has its separate issues and different objectives.

In the Phase I study [13], the comparative heat transfer performance of CFC-114 and HFC-236ea was determined for a plain tube and two types of integral finned tubes (1024-fpm and 1575-fpm tubes) during condensation and pool boiling.

In the Phase II study, the heat transfer performance of HFC-236ea during condensation, pool boiling, and spray evaporation was evaluated for high performance enhanced tubes (Turbo-CII, Turbo-B, and Turbo-BII tubes). The report on this study is being prepared.

In the study reported here (Phase III), the heat transfer coefficients of HFC-236fa during condensation and pool boiling were determined for both the integral finned tubes previously evaluated in Phase I [13] and the high

performance enhanced tubes evaluated for HFC-236ea in Phase II. Comparisons with results from Phase I and Phase II are also made here in Chapter 5 for the condensation work and Chapter 6 for the pool boiling work.

The hermetically sealed compressors in vapor compression refrigeration systems require lubricant to protect moving components. However, a small amount of the lubricant is entrained with refrigerant leaving the compressor and circulates through the whole system. The oil carried with refrigerant might significantly affect the performance of evaporators since the oil concentration in the liquid mixtures increases when the volatile refrigerant is evaporated and the non-volatile oil is left in the evaporators. The effects of additional oil on pool boiling were investigated for CFC-114 (Phase I), HFC-236ea (Phase I), and HFC-236fa (Phase III). Results are discussed in Chapter 6.

Since no general theoretical correlations exist to predict heat transfer coefficients as a function of either refrigerant type, tube surface geometry, or lubricant addition, experiments are the most reliable means to determine the heat transfer coefficients for specific applications.

RESEARCH PROGRAM

Objectives

This study not only measured the shell-side heat transfer coefficients of an environmentally safe refrigerant, HFC-236fa, during condensation and pool boiling for two integral finned tubes (1024-fpm and 1575-fpm tubes) and three high performance enhanced (Turbo-CII, Turbo-B, and Turbo-BII) tubes but also compared the heat transfer performance of the tubes tested with HFC-236fa. In addition, the comparison of the heat transfer coefficients for HFC-236fa, HFC-236ea and CFC-114 was also an important objective, where the two HFC refrigerants are proposed as alternative refrigerants for CFC-114.

Scope

Using the same test facility which allows analysis of condensation and pool boiling, measurements were conducted on a single-tube configuration at a saturation temperature of 2°C for pool boiling and at 40°C for condensation. The testing range of heat fluxes was from 15 kW/m^2 to 40 kW/m^2 for both condensation and pool boiling.

The heat transfer coefficients of HFC-236fa were tested for two types of integral finned tubes (1024-fpm and 1575-fpm tubes) and three types of high performance enhanced tubes (Turbo-CII, Turbo-B, and Turbo-BII tubes). The 1024-fpm tube is presently used in Navy shipboard heat exchangers to enhance heat transfer. However, the 1575-fpm tube and the three high performance enhanced tubes which were produced by advanced manufacturing techniques have not been used in the shipboard chillers. In this study, the two integral finned tubes

were tested for both condensation and pool boiling. In addition, the condensation enhanced Turbo-CII tube was tested during shell-side condensation while the evaporation enhanced Turbo-B and Turbo-BII tubes were tested in pool boiling.

High performance enhanced tubes with improved heat transfer characteristics and with complex fin profiles are widely used in heat exchangers for refrigeration and air-conditioning applications, and, therefore, are potential replacements for the integral finned tubes presently used in Navy shipboard chillers. The heat transfer coefficients for the integral finned tubes were used as a baseline for comparing the heat transfer performance of the high performance enhanced tubes. All tubes compared had an equivalent tube diameter of 19.1 mm (3/4 in.).

The heat transfer results for CFC-114, HFC-236ea, and HFC-236fa were compared. In addition, the heat transfer performance of the high performance enhanced tubes was compared with the integral finned tubes for HFC-236ea in Phase II and for HFC-236fa in this study (Phase III). The effects of oil in the refrigerant on the heat transfer performance during pool boiling were assessed for CFC-114 and HFC-236ea in Phase I and for HFC-236fa in this study (Phase III).

The data taken in this study were obtained using the same test facility as previously used in Phase I [13] and Phase II. Data were taken with increasing heat loads during condensation and with decreasing heat loads during pool boiling. Each tube type was tested twice on two different days in order to test the accuracy and repeatability of the system.

Data are mainly presented in the form of heat transfer coefficient versus heat flux, since the heat transfer coefficient during condensation and pool boiling depends on the heat load.

CHAPTER 2

CONCLUSIONS

The heat transfer coefficients of HFC-236fa (proposed as a CFC-114 substitute) were measured for two integral finned tubes (1024-fpm and 1575-fpm tubes) and three high performance enhanced tubes (Turbo-CII, Turbo-B, and Turbo-BII tubes) during shell-side condensation and pool boiling on the outside of a single horizontal tube.

The high performance enhanced tubes were found to effectively increase heat transfer and produced higher heat transfer coefficients than the integral finned tubes. The results tested previously in Phase I [13] and Phase II showed the same trend.

During shell-side condensation, the Turbo-CII tube produced noticeably higher heat transfer coefficients than the 1024-fpm and 1575-fpm tubes, while the two finned tubes were found to have similar performance. The Turbo-CII tube yielded 1.2 to 1.8 times the heat transfer coefficients of the 1024-fpm tube and 1.4 to 1.7 times the values of the 1575-fpm tube.

The pool boiling results for both pure HFC-236fa and for HFC-236fa with oil show that the tube performance in descending order was Turbo-BII tube, Turbo-B tube, 1024-fpm tube, and 1575-fpm tube. Heat transfer coefficients of pure HFC-236fa provided by the Turbo-B tube were 1.6 to 1.7 and 1.9 to 2.2 times those by the 1024-fpm tube and the 1575-fpm tube, respectively. The Turbo-BII tube outperformed the other tubes tested and produced 1.2 to 1.8 times the heat transfer coefficients of the Turbo-B tube.

For the pool boiling testing, a miscible polyol-ester oil was added to HFC-236fa with the oil concentrations of 1% and 3% by weight. This polyol-ester oil (Castrol Icematic SW-68) is a commercial lubricant with a viscosity of 340 SSU at 37.8°C (100°F). The oil in HFC-236fa caused the boiling coefficients to deviate less than 10% from the pure HFC-236fa results for all the tubes tested except the Turbo-BII tube.

Although the Turbo-BII tube produced the highest heat transfer coefficients of all the tubes tested, it showed larger changes in pool boiling performance with the addition of oil. Specifically, the Turbo-BII tube gave a 10% to 30% increase at the 1% oil concentration over the results for pure HFC-236fa and a 10% decrease to 15% increase at the 3% oil concentration.

A comparison of shell-side heat transfer coefficients was made for CFC-114 and its two proposed alternative refrigerants, namely, HFC-236fa and HFC-236ea. In general, HFC-236fa was found to have better heat transfer performance than CFC-114 and HFC-236ea for both shell-side condensation and pool boiling.

The average increase in condensation heat transfer coefficients for HFC-236fa compared to CFC-114 was 30% for the 1024-fpm tube and 20% for the 1575-fpm tube, while compared to HFC-236ea the average increase with HFC-236fa was 20% for both the 1024-fpm and 1575-fpm tubes. The heat transfer performance of the Turbo-CII tube tested with HFC-236fa was similar to or slightly lower (average less than 5%) than that with HFC-236ea.

The average increase in pool boiling heat transfer with HFC-236fa compared to CFC-114 was 60% for the 1024-fpm tube and 50% for the 1575-fpm tube, while compared to HFC-236ea the average increase with HFC-236fa was 10% for both the 1024-fpm and 1575-fpm tubes and 50% for both the Turbo-B and Turbo-BII tubes.

Replacing CFC-114 with HFC-236fa is desired in terms of the comparative heat transfer performance of CFC-114, HFC-236ea, and HFC-236fa made in this study. In addition, the attraction of the high heat transfer offered by the high performance enhanced tubes should be weighed against degraded heat transfer with increasing oil concentrations possibly occurring in operational evaporators. The high performance enhanced tubes outperformed the ordinary finned tubes at all the testing conditions in this research, including oil concentrations up to 3% in HFC-236fa.

CHAPTER 3

RECOMMENDATIONS

Recommendations for future research in the heat transfer evaluation of alternative refrigerants for CFC-114 or other CFCs are listed as follows:

1. Compare the data for alternative refrigerants with the existing heat transfer correlations and derive new ones.
2. Apply understanding of fundamentals to develop analytical models for two-phase heat transfer for complex surface geometries.
3. Investigate the effects of oil with larger concentrations (above 3%) in refrigerant on pool boiling performance, and seek a plausible accepted theory to explain the boiling phenomena observed in oil/refrigerant mixtures.
4. Test the other enhanced tubes made or suggested by different manufacturers and other researchers.

CHAPTER 4

EXPERIMENTAL DESCRIPTION

EXPERIMENTAL APPARATUS

Even though the same test rig was used in all the experiments, different experimental arrangements were required for testing condensation and pool boiling. The schematics of the experimental arrangements for testing these two heat transfer modes are shown in Figures 4.1 and 4.2, respectively. The main components of the test facilities include the test section, test tubes, closed water loop, closed refrigerant loop, glycol/water chiller, and data acquisition system.

The heat transfer experiments were performed in a cylindrical, stainless steel chamber equipped with sight glasses in the front and the rear wall for allowing observation of heat transfer phenomena. On the top of the test section were two ports which are passageways for vapor. The test section also had two other ports on the bottom to serve as liquid paths. Two tube sheets with threaded ports are attached to both ends of the cylindrical chamber so that the tube can be changed by adjusting the compression fittings.

The tubes tested were copper alloy and had a 19.1-mm (3/4-in.) nominal outside diameter and external enhanced surface geometries. The inner tube surface of the high performance enhanced tubes was grooved by the manufacturer for increasing the in-tube heat transfer coefficient. In addition, a spring-type turbulator was inserted inside each tube tested to promote continuous turbulence and thus balance the thermal resistance on both sides of the tube. The turbulator was provided by the Trane Company located in La Crosse, Wisconsin and made of a wire coil with such a diameter that can be held at the inner tube surface by the friction fit between the stretched spring and the tube wall. The geometric specifications of the tubes tested are given in Table B.1 in SI units and Table B.2 in English units. All tubes tested were supplied by Wolverine Tube, Inc., Decatur, Alabama. The readers can refer to the company for more detailed information on these tubes.

Both the 1024-fpm and 1575-fpm tubes are integral low-fin tubes. The 1024-fpm tube has a fin density of 26 fins per inch and the 1575-fpm tube has 40 fins-per-inch. Furthermore, the fin height value of the 1024-fpm tube is about 70% greater than the 1575-fpm tube. Basically, all the high performance enhanced tubes evaluated here are made by deforming or modifying low-fin tubes and have complex, outward enhanced surface geometries. The Turbo-CII tube has short roughened fins, and the Turbo-B and Turbo-BII tube are characterized by reservoir-type (or re-entrant) cavities with narrow openings constructed by the compressed, doubly cut knurl.

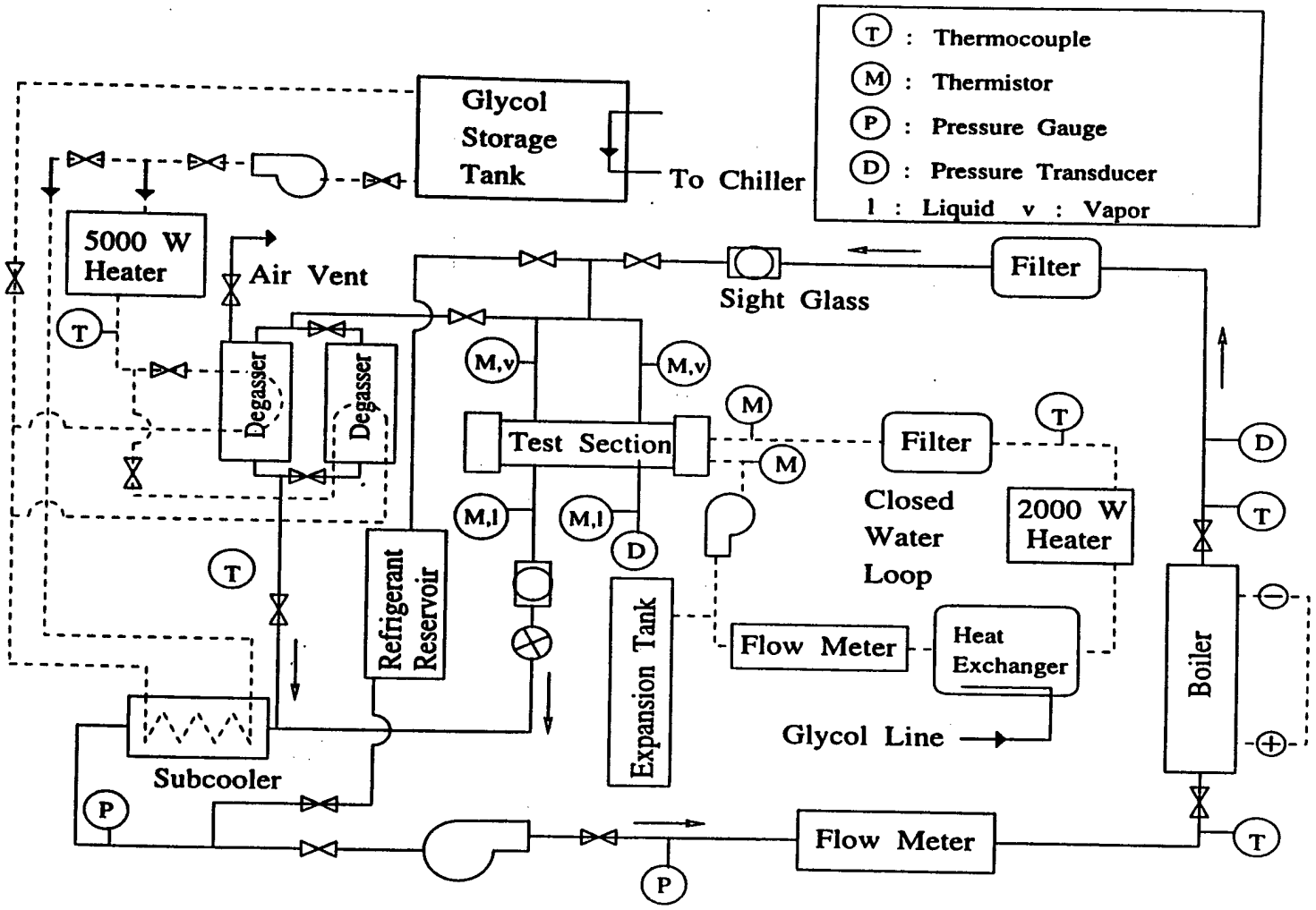

Figure 4.1: Schematic of test facility for condensation tests.

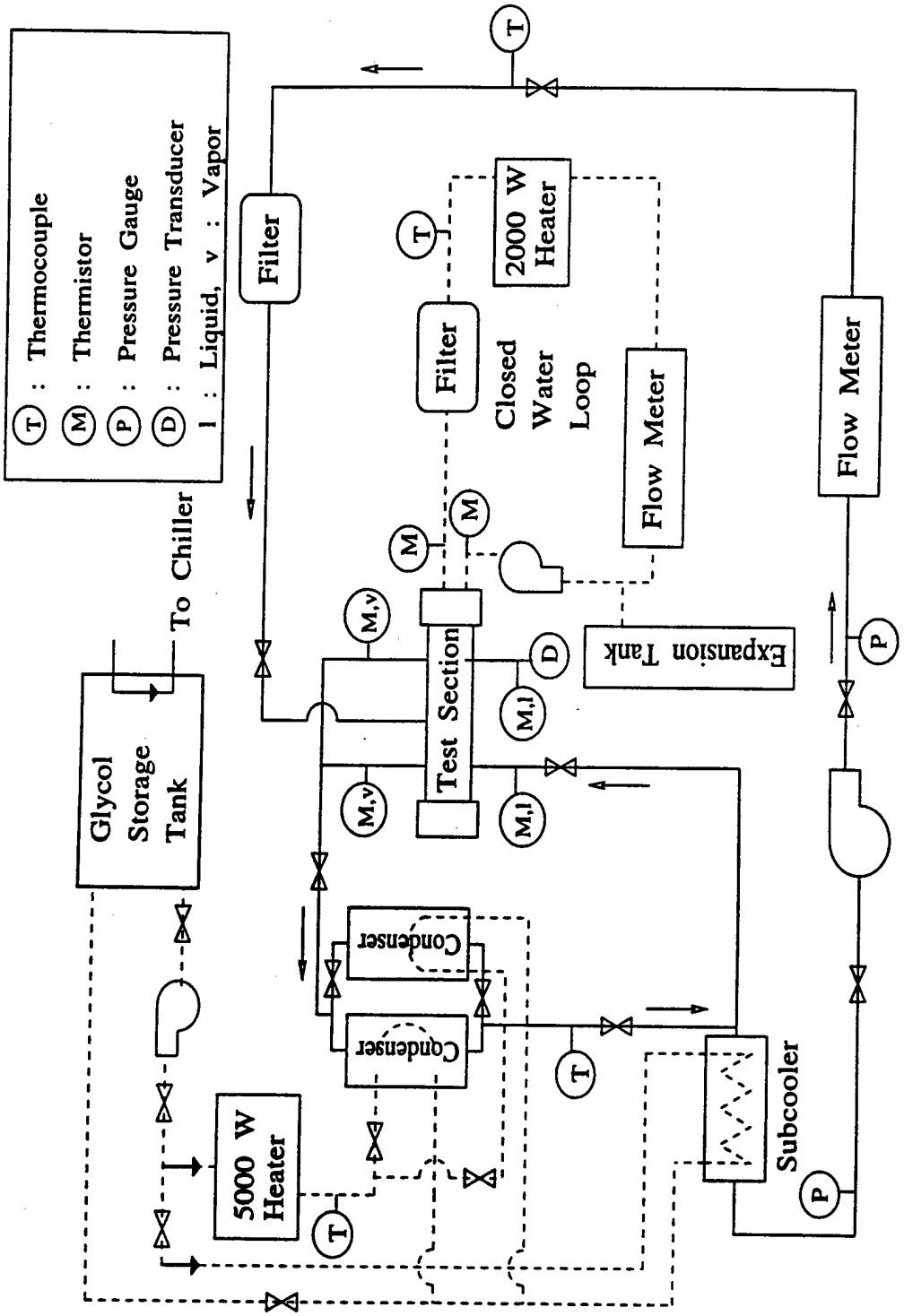

Figure 4.2: Schematic of test facility for pool boiling tests.

The design of the Turbo-B tube is based on a 1575-fpm tube, whereas the Turbo-BII tube is based on a 1969-fpm (50-fpi) tube. The higher fin density of the Turbo-BII tube provides a higher density of nucleation sites. In addition, the boiling sites of the Turbo-BII tube are shape-optimized for specific types of refrigerants, while those of the Turbo-B tube are not. The Turbo-CII tube is designed to enhance shell-side condensation, while the Turbo-B and Turbo-BII tubes are designed to improve nucleate boiling.

The closed water loop consists mainly of a storage tank, two triplex diaphragm pumps, a flow meter, an immersion heater, and a dual-tube heat exchanger. The heater and heat exchanger were used to control the water temperature.

The glycol/water mixture was pumped through a chiller of 105-kW (30-ton) cooling capacity and could be supplied to a dual-tube heat exchanger, two condensers, and a subcooler through manifolds.

While water was circulated in the test tube, refrigerant was delivered by a triplex diaphragm pump to the test section through several routes with different auxiliary facilities for different purposes. During condensation tests, a stainless steel boiler was used to vaporize refrigerant before it reached the test section. For evaporation tests, a subcooler and two condensers were utilized to condense refrigerant after it was boiled in the test section.

A detailed description of the apparatus can be found in Huebsch and Pate [13].

INSTRUMENTATION AND CALIBRATION

The temperatures necessary for calculating the shell-side heat transfer coefficient were measured by thermistors and compared with the saturation temperature corresponding to the measured pressure. The acceptable difference in these two temperatures was within ± 0.2°C for condensation tests, and ± 0.1°C for evaporation tests.

Due to the low pressures of HFC-236fa and the low operating temperatures for the evaporation tests (see Appendix A), the strain-gauge pressure transducer which had been used to measure the saturation pressure of the test section was sent to the Setra Company and calibrated professionally instead of being calibrated by a simple dead-weight tester. The thermistors were also re-calibrated by using a constant temperature bath. Lack of scatter found in the calibration results indicates the consistency of the calibration.

The instrumentation accuracy is ± 0.05°C for the thermistors, ± 0.1% of the full scale for the pressure transducer, and ± 0.20% of the full scale for the water mass flow meter.

EXPERIMENTAL PROCEDURES

Procedures for condensation testing

After the system was verified to be leak-free, it was evacuated by a vacuum pump for 8 hours. Subsequently, the refrigerant was charged into the system. The noncondensible gas in the system was purged through the vent valves on the top of the degassers (condensers) while the refrigerant was boiling in the test section. This degassing procedure was repeated until the temperatures registered by the thermistors were within 0.2°C of those corresponding to the saturation temperature read by the pressure transducer. The condensers were isolated once the purging had been done.

The liquid refrigerant delivered from the pump was converted to vapor in a boiler and then condensed by the cooler water flowing through the test tube. The refrigerant condensed in the test section flowed back to the pump and was recirculated. With flows established, the water and refrigerant flow rates along with the temperatures of the refrigerant in the boiler and water were adjusted to meet the required energy rate balance and maintain the refrigerant saturation temperature of 40°C in the test section. Meanwhile, the temperature change of water through the test section was maintained at 2°C. Temperatures of water flowing inside the test tube were controlled by a heater and a heat exchanger where the glycol/water mixture (coolant) was circulated through it.

The flow rates of the two fluids (water and refrigerant) and the temperatures of the refrigerant in the boiler and water were adjusted to meet the different heat transfer requirements over the whole range of heat fluxes tested.

Procedures for pool boiling testing

The refrigerant was boiled by the circulating warm water in the test section and condensed in the condensers where the glycol/water mixture (coolant) was circulated and then returned to the pump. The refrigerant temperature was maintained at a steady state value of 2°C by controlling the flow rates and temperatures of the water and coolant. The water flowing inside the test tube was heated by a heater, and the water temperature change through the test tube was controlled at 2°C. In addition, the two condensers were adjusted to work independently or in parallel for the different heat load requirements.

The flow rates and temperatures of the water and coolant to meet the different heat transfer requirements were adjusted to provide the whole range of heat fluxes.

A detailed description of experimental procedures for condensation and pool boiling is given by Huebsch and Pate [13].

DATA REDUCTION

The average shell-side heat transfer coefficient (h) for a single-row tube with two passes arranged side by side was determined using the energy rate balance between the two fluids (refrigerant and water), where a logarithmic mean temperature difference (LMTD) method was applied. The measured parameters for calculating shell-side heat transfer coefficients were the temperatures of water entering and leaving the test section, the refrigerant saturation temperature and pressure of the test section, and the flow rates of water and refrigerant.

The heat flux applied to the refrigerant was controlled throughout the experiments to obtain the average shell-side heat transfer coefficient. The testing range of heat fluxes was from 15 kW/m^2 to 40 kW/m^2 for both condensation and pool boiling.

A modified Wilson plot method was used to determine the in-tube heat transfer coefficient, and then the average shell-side heat transfer coefficient was calculated from the UA-value by applying the LMTD approach. Under steady state conditions, the heat transfer rate (q, W) between the refrigerant and the water is formulated as,

$$q = U_o \cdot A_o \cdot LMTD \tag{4.1}$$

where the heat transfer rate (q, W) was calculated (Equation 4.2) from the measured inlet and outlet temperatures of water ($T_{i,in}$ and $T_{i,out}$, °C), specific heat of water (Cp_i, J/kg·K), and water flow rate ($\dot{m}_i$, kg/s),

$$q = \dot{m}_i \cdot Cp_i \cdot (T_{i,out} - T_{i,in}) \tag{4.2}$$

The logarithmic mean temperature difference (LMTD, °C) in Equation 4.1, defined by Equation 4.3, was obtained from the measured refrigerant saturation temperature in the test section (T_{sat}, °C) and the water temperatures entering and leaving the test section ($T_{i,in}$ and $T_{i,out}$, °C).

$$LMTD = \frac{(T_{i,out} - T_{i,in})}{\ln \dfrac{(T_{sat} - T_{i,in})}{(T_{sat} - T_{i,out})}} \tag{4.3}$$

Obtaining q from Equation 4.2 and LMTD from Equation 4.3 and re-arranging Equation 4.1, the overall heat transfer coefficient (U_o, W/m^2·K) based on the outside tube surface area (A_o, m^2) was computed from

$$U_o = \frac{q}{A_o \times LMTD} \tag{4.4}$$

The shell-side heat transfer coefficient (h, W/m^2·K) was then determined from the overall heat transfer coefficient by subtracting the tube-wall thermal resistance (R_w, K/W) and the forced convective heat transfer coefficient (h_i, W/m^2·K) on the water side using

$$h = \frac{1}{\frac{1}{U_o} - \frac{A_o}{A_i}\frac{1}{h_i} - A_o R_w} \tag{4.5}$$

The tube-wall thermal resistance (R_w, K/W) in Equation 4.5 is given by

$$R_w = \frac{\ln(D_o / D_i)}{2\pi k_w L} \tag{4.6}$$

and the in-tube heat transfer coefficient (h_i) was calculated by the Sieder-Tate equation listed below and deduced by a modified Wilson plot technique.

$$h_i = STC \cdot \frac{k_i}{D_i} Re_i^{0.8} Pr_i^{0.33} \left(\frac{\mu_i}{\mu_w}\right)^{0.14} \tag{4.7}$$

The thermal conductivity of tube wall (k_w, W/m·K) in Equation 4.6 and the viscosity of water (μ_w, N·s/m^2) in Equation 4.7 were calculated using the tube wall temperature ($T_w = (T_{sat}+T_{i,bulk})/2$, °C). The Reynolds number (Re_i), Prandtl number (Pr_i), thermal conductivity (k_i, W/m·K), and dynamic viscosity (μ_i, N·s/m^2) in Equation 4.7 were based on the average bulk temperature ($T_{i,bulk} = (T_{i,in}+T_{i,out})/2$, °C) and properties of water. The remaining parameters in the equations above L (m), D_i (m), D_o (m), and A_i, (m^2), are the tube length, inside tube diameter, outside tube diameter, and inner surface area of the tube, respectively.

Based on the modified Wilson plot technique, the constant STC (Sieder-Tate coefficient) required in Equation 4.7 was determined by boiling refrigerant at a constant heat load of 1.5 kW and maintaining a constant saturation temperature of 2°C on the outside of the tested tube while varying the in-tube water flow rate.

The following equation was generalized by substituting Equation 4.7 for h_i into the equation of thermal resistance (Equation 4.5):

$$Y = \frac{1}{STC} \cdot X + \frac{1}{h} \tag{4.8}$$

where

$$Y = \frac{1}{U_o} - A_o R_w \tag{4.9}$$

$$X = \frac{A_o / A_i}{\frac{k_i}{D_i} Re_i^{0.8} Pr_i^{0.33} \left(\frac{\mu_i}{\mu_w}\right)^{0.14}} \tag{4.10}$$

The range of the Reynolds number tested for water was from 2800 to 19000 for the finned tubes and from 2800 to 18000 for the high performance enhanced tubes. Corresponding to the different water flow rates, the plotted Y (m^2·K/W) values versus X (m^2·K/W) values form a linear curve. As indicated in Equation 4.8, the STC is the inverse of the slope of the plotted X-Y curve. The constant STC value was found to be 0.0471 for the 1024-fpm tube, 0.0514 for the 1575-fpm tube, 0.131 for the Turbo-B tube, 0.108 for the Turbo-BII tube, and 0.1138 for the Turbo-CII tube.

The numerical values for all the data obtained in this study are tabulated in Appendix C.

EXPERIMENTAL UNCERTAINTY OF DATA

Uncertainty for the shell-side heat transfer coefficients in the present study was calculated by using the uncertainty analysis described in the Phase I report [13]. The uncertainty in the calculated heat transfer coefficients is listed in Table 4.1 for the condensation data and Table 4.2 for the pool boiling data. Appendix D presents the derivation of uncertainty analysis equations for the calculated shell-side heat transfer coefficients.

It is important to balance the thermal resistance on both sides of a test tube. The uncertainty of the shell-side heat transfer coefficients was found to be smaller when the tube side had a denser turbulator (i.e., a more flow restricting device) inserted because it enabled a higher heat transfer coefficient with water flowing inside the tube.

TABLE 4.1: UNCERTAINTY IN THE SHELL-SIDE HEAT TRANSFER COEFFICIENTS FOR CONDENSATION

	Uncertainty		
Heat flux	15 kW/m^2	30 kW/m^2	40 kW/m^2
1024-fpm tube	± 9%	± 6%	± 6%
1575-fpm tube	± 8%	± 6%	± 6%
Turbo-CII tube	±7%	± 6%	± 5%

TABLE 4.2: UNCERTAINTY IN THE SHELL-SIDE HEAT TRANSFER COEFFICIENTS FOR POOL BOILING

	Uncertainty		
Heat flux	15 kW/m^2	30 kW/m^2	40 kW/m^2
1024-fpm tube	± 10%	± 8%	± 7%
1575-fpm tube	± 8%	± 7%	± 6%
Turbo-B tube	± 11%	± 9%	± 7%
Turbo-BII tube	± 19%	± 11%	± 9%

CHAPTER 5

CONDENSATION RESULTS

OVERVIEW

Condensation is defined as the conversion from the vapor to liquid phase by the removal of latent heat from a substance. When refrigerant vapor contacts cooler tubes below the vapor's saturation temperature, condensate is formed on the tubes and the liquid acts as a resistance to heat transfer on the tube surface. Then the accumulated condensate falls from the bottom of horizontal tubes as droplets, columns, or sheets. The drainage patterns in bundles of different tube types were observed by Webb and Murawski [26] in their study of the row effects due to condensate loading.

Condensation heat transfer on a horizontal tube with rough surfaces is mainly subject to the combined effects of surface tension, gravitational force, and tube surface geometry. While surface tension plays the predominant role during condensation of stagnant vapor on rough surfaces such as finned construction [4], the effects of vapor shear stress at the phase interface may dominate the falling mode of condensate in the presence of a large vapor velocity.

Most of the theoretical models developed for condensation on finned tubes considered only the effects of gravity, surface tension, and fin efficiency [1], [16], [18], while some recent experiments were conducted on variety of finned tubes to assess the effects on condensation heat transfer of vapor shear stress at the liquid-vapor interface [2], [4], [5], [6].

The removal mechanism of condensate is closely related to the geometrical characteristics of tube surfaces. Numerous studies that investigated the effects of fin density and geometry on condensation heat transfer performance of horizontal finned tubes have been reported [3], [8], [9], [19]. Three tubes with two distinctively different geometries, which include a high performance enhanced tube (Turbo-CII tube) and two integral finned tubes (1024-fpm and 1575-fpm tubes), were tested with HFC-236fa in this study. Their heat transfer performance is compared not only with each other but also with the previous results for CFC-114 and HFC-236ea in the following sections.

Other parameters, such as the influence of noncondensable gases in the condensing vapor which can decrease condensation heat transfer, were studied by Ullmann and Letan [21].

CONDENSATION RESULTS FOR HFC-236fa

Figure 5.1 shows that the dependence of the heat transfer coefficient on the heat flux for the tubes tested (1024-fpm, 1575-fpm, and Turbo-CII tubes). As the heat flux increased, the heat transfer coefficients increased for these three tubes. Condensation data published by Huber et al. [12] and Huebsch and Pate [13] showed similar trends.

The high performance Turbo-CII tube performed better than the 1024-fpm and 1575-fpm tubes. Specifically, the Turbo-CII tube provided an increase in heat transfer coefficient around 20% to 80% with respect to the 1024-fpm tube and about 40% to 70% with respect to the 1575-fpm tube.

In another investigation [10] [11] which tested these three tubes but with HFC-134a, the heat transfer coefficients produced by the Turbo-CII tube were found to be approximately two to three times larger, based on the average bundle data, than those of the 1024-fpm and 1575-fpm tubes, while for the first-row data the values were around three times larger than the 1024-fpm tube and two times larger than the 1575-fpm tube.

Figure 5.1 also reveals that the two integral finned tubes produced similar heat transfer coefficients which were relatively insensitive to the change of heat flux. Conversely, the Turbo-CII tube yielded a sharp change in the heat transfer coefficient with increasing heat flux. These results are consistent with those reported by Huber et al. [11], which also indicated that the decrease in the heat transfer coefficient with increasing heat load was more dramatic for the Turbo-CII tube than for the two finned tubes.

Figure 5.2 shows that the heat transfer coefficient for HFC-236fa depends on the difference between the refrigerant saturation temperature and the tube-wall temperature for shell-side condensation. It can be observed that for the Turbo-CII tube small temperature differences yielded higher heat transfer coefficients at a given heat flux. Figure 5.2 also shows that the heat transfer coefficients for the finned tubes were nearly constant over the evaluated range of the condensation temperature differences.

Figure 5.2 also shows the variation of heat transfer coefficients with the temperature difference across the condensate film. As the condensation temperature difference increased, the heat transfer coefficients increased for the Turbo-CII tube and slightly increased for the two finned tubes.

The data for the repeatability run can be seen in Figures 5.1 and 5.2. Because of the closeness of the data for the primary run and repeat run, they are not distinguished in the figures. Both runs were taken in steps from low heat flux to high heat flux, but on different days.

COMPARISON WITH AN EXISTING CORRELATION

Most of the existing equations were developed for condensation on tubes with rectangular or trapezoidal cross-section fins [1], [16], [18]. A model published by Webb and Murawski [26] was used to compare the condensation data obtained in the current study for the 1024-fpm, 1575-fpm, and Turbo-CII tubes, since this model

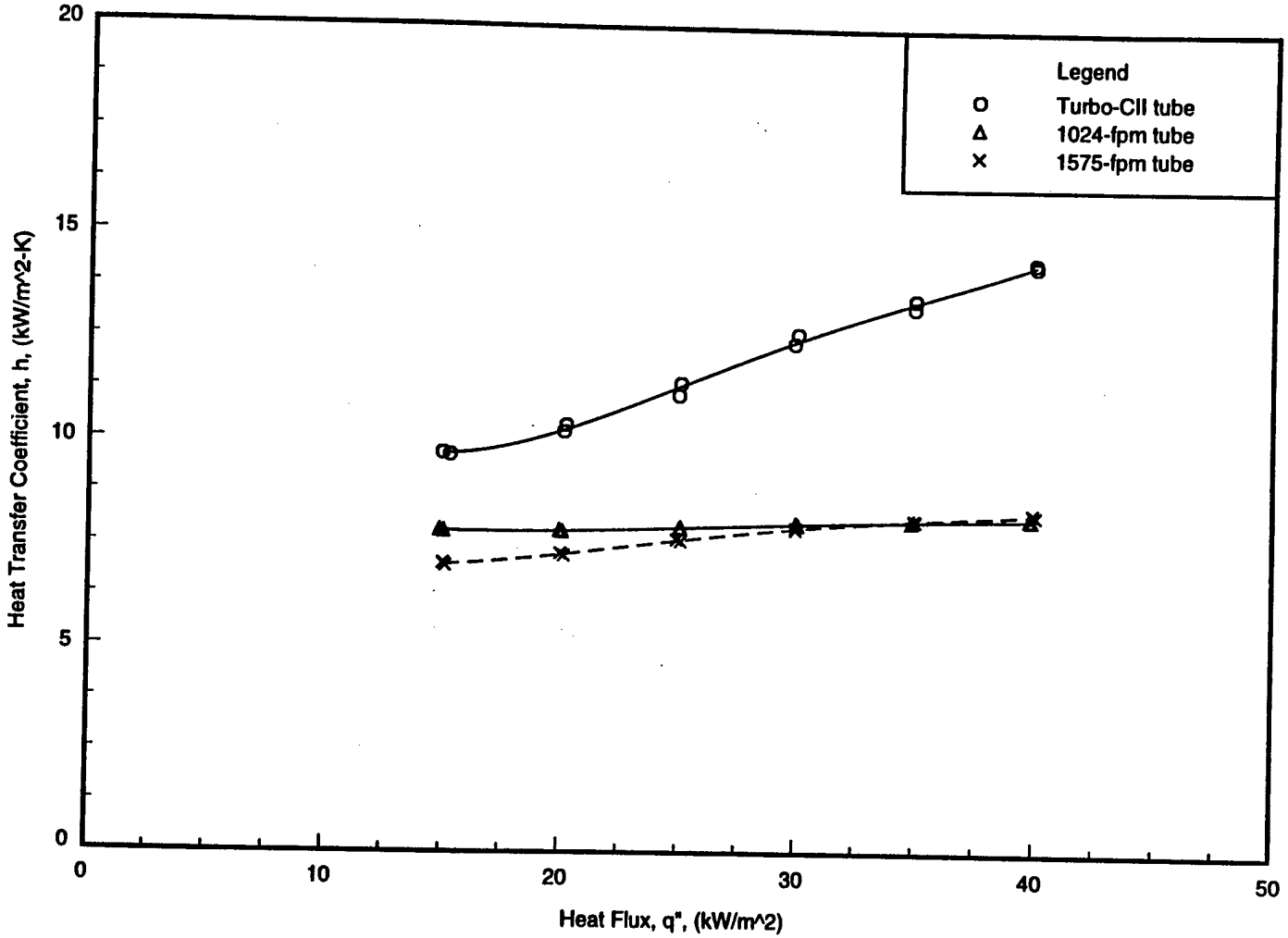

Figure 5.1. Condensation heat transfer coefficients for HFC-236fa using the Turbo-CII, 1024-fpm, and 1575-fpm tubes at T_{sat} = 40°C.

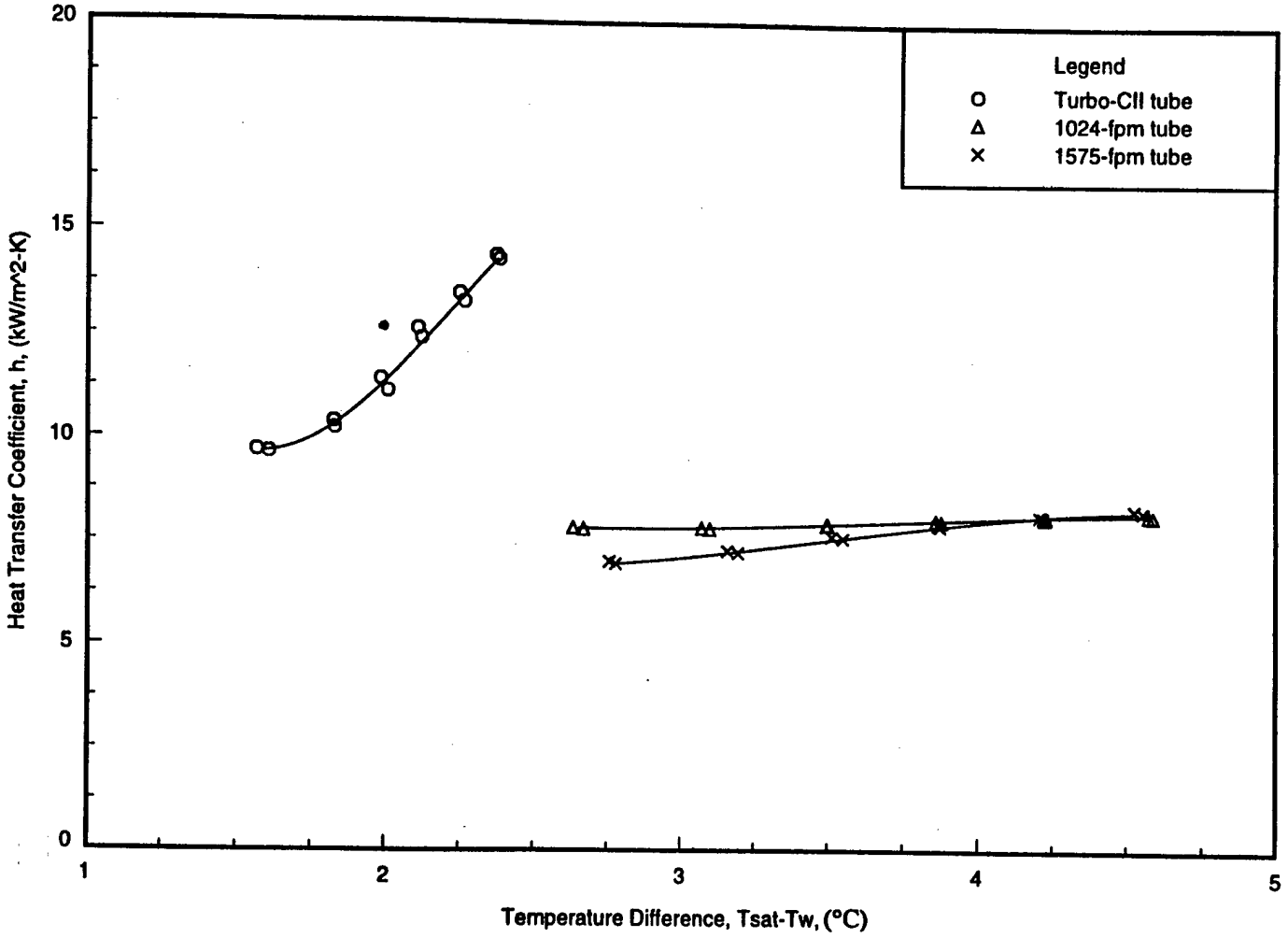

Figure 5.2. Temperature difference effects on condensation heat transfer coefficients for HFC-236fa at T_{sat} = 40°C.

was derived for the condensation heat transfer coefficients of CFC-11 on five enhanced tube types which included one integral finned tube and four enhanced tubes with distinctly different, complex fin profiles.

Webb and Murawski reported that the heat transfer coefficient for the Nth tube row (h_{NR}, W/m^2·K) is only a function of the condensate Reynolds number leaving the Nth tube row (Re_{NR}),

$$h_{NR} = a \cdot Re_{NR}^{-n} \tag{5.1}$$

The average condensation coefficient (h_N, W/m^2·K) for a bundle of N tube rows was obtained by integrating Equation 5.1 from the first row to the Nth row,

$$h_N = [\frac{a}{1-n}(Re_{NR} - Re_1)][(Re_{NR})^{1-n} - (Re_1)^{1-n}] \tag{5.2}$$

where the Reynolds number for film condensation on tubes is defined as,

$$Re = \frac{4 \cdot \Gamma}{\mu} \tag{5.3}$$

The parameters Re_1, Re_N, Γ, and μ are the condensate Reynolds numbers leaving the first row and the Nth row, condensate mass flow rate per unit tube length (kg/m-s), and dynamic viscosity of condensate (kg/m-s), respectively. The constants a and n shown in Equations 5.1 and 5.2 correspond to 257800 W/m^2·K and 0.507, for the Turbo-C tube, and 13900 W/m^2 K and 0. for the 1024-fpm tube. These constants were obtained by curve fitting the experimental data for h_{NR} versus Re_{NR}. The data for the Turbo-CII tube and the two finned tubes were compared with the Webb-Murawski correlation using the constants derived for the Turbo-C tube and for the 1024-fpm tube, respectively. The constants for the other different tubes can be found in the original paper [26].

As shown in Figures 5.3 and 5.4, the model values are higher than the empirical results. The data lines for the two finned tubes almost parallel the correlation. While the predicted values for the Turbo-CII tube agree with the measured data at the highest heat flux of 40 W/m^2, they show an increasing deviation with decreasing heat flux. The 1024-fpm tube, 1575-fpm tube, and Turbo-CII tube provided heat transfer coefficients approximately 1.7, 1.7 to 2.0, and 1.0 to 2.4 times as large as predicted by the Webb-Murawski correlation.

Using the Webb-Murawski correlation and constants for the Turbo-C tube, the average heat transfer coefficients of HFC-236ea measured for the Turbo-CII tube in Phase II were found to be 30% to 70% less than the predicted values. Using the same correlation and constants for the Turbo-C tube, the average heat transfer

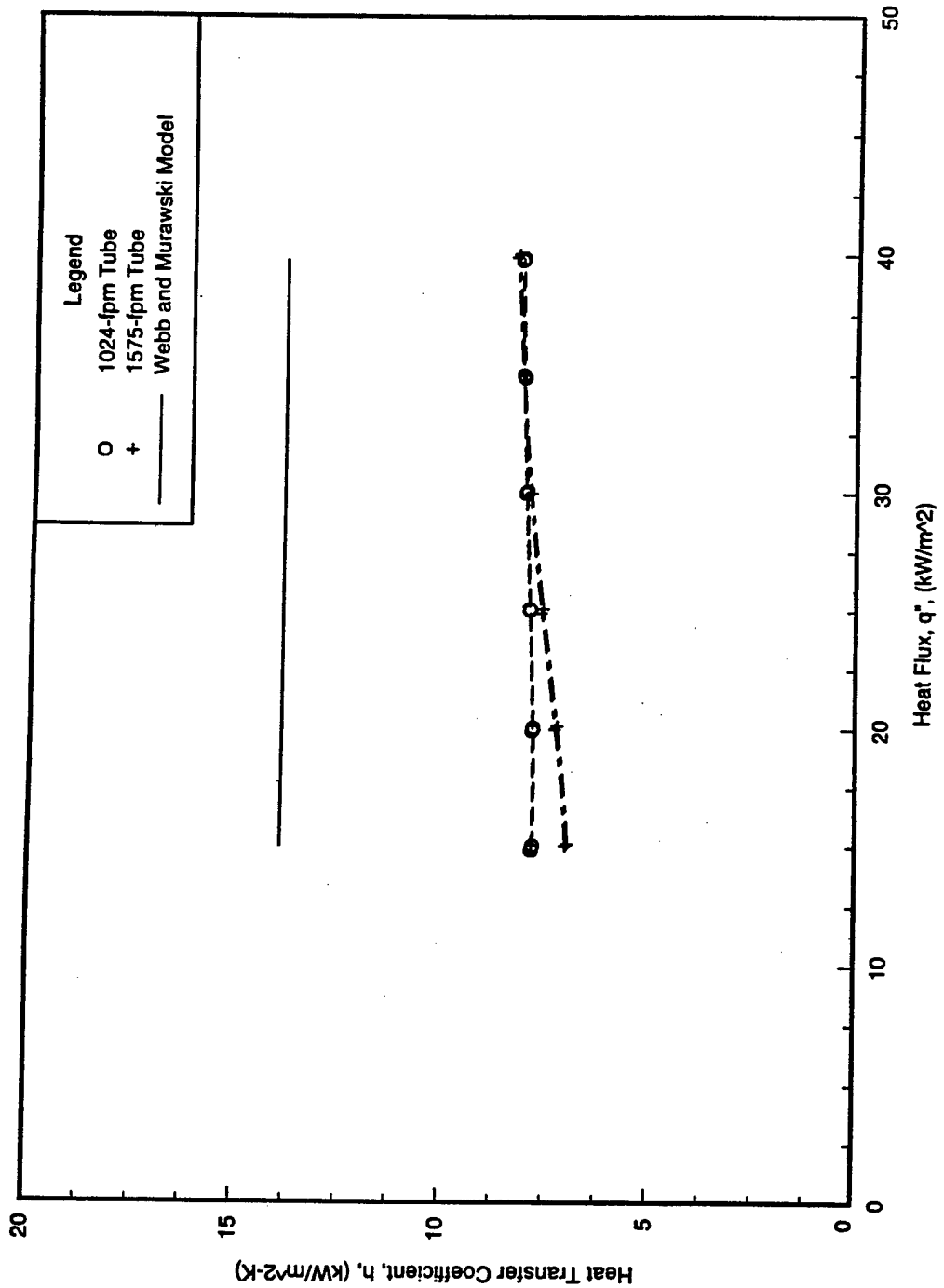

Figure 5.3. Correlation comparison of HFC-236fa for the 1024-fpm and 1575-fpm tubes (tube dia. = 19.1 mm) at T_{sat} = 40°C.

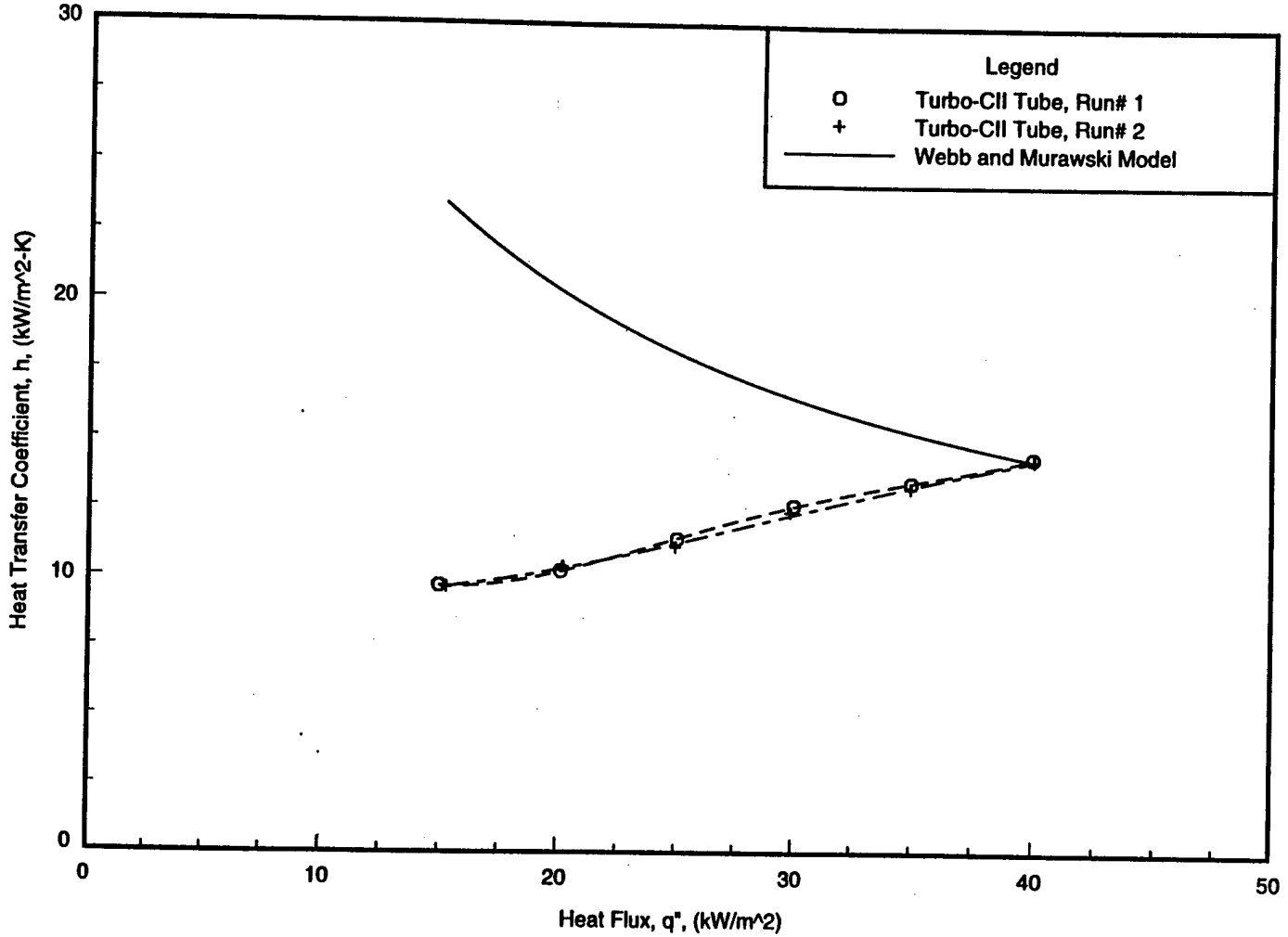

Figure 5.4. Correlation comparison of HFC-236fa for the Turbo-CII tube (tube dia.= 19.1 mm) at T_{sat} = 40°C.

coefficients measured by Huber et al. [12] for the Turbo-CII tube were three to four times and 20% higher than the predicted values for HFC-134a and HCFC-123, respectively. The authors attributed the poor agreement between the empirical and model results to the different refrigerants tested.

COMPARISON OF RESULTS FOR CFC-114, HFC-236ea, AND HFC-236fa

Condensation heat transfer coefficients for HFC-236fa, CFC-114, and HFC-236ea were compared in Figures 5.5 through 5.7 for the 1024-fpm tube, 1575-fpm tube, and Turbo-CII tube, respectively. In general, higher heat transfer coefficients were obtained with HFC-236fa than with CFC-114 or HFC-236ea for the two finned tubes.

For the 1024-fpm tube, the heat transfer coefficients of HFC-236fa were around 30% to 40% higher than those of CFC-114 and 10% to 30% higher than those of HFC-236ea. For the 1575-fpm tube, the heat transfer coefficients of HFC-236fa were around 20% to 30% higher compared to.CFC-114 and 10% to 30% higher compared to HFC-236ea. For the high performance Turbo-CII tube, the heat transfer coefficients of HFC-236fa were found to be similar to or slightly lower (average less than 5%) than those of HFC-236ea. The performance of HFC-236fa and HFC-236ea was reversed on this tube compared with the finned tubes. These reversed results might indicate that the distinctively different surface geometry of the Turbo-CII tube from that of the finned tubes had a significant effect on the performance of these refrigerants. Data were not taken on the Turbo-CII tube with CFC-114.

SUMMARY

Heat transfer coefficients are presented for condensation of HFC-236fa on three tube types: a 1024-fpm tube, a 1575-fpm tube, and a Turbo-CII tube. A comparison was also made for these tubes with the previous results of CFC-114 and HFC-236ea obtained in the same test facility.

The best condensation heat transfer performance with HFC-236fa was provided by the high performance Turbo-CII tube with an increase in heat transfer coefficients around 20% to 80% with respect to the 1024-fpm tube and about 40% to 70% with respect to the 1575-fpm tube.

HFC-236fa performed better than CFC-114 and HFC-236ea during condensation for all tubes tested except the Turbo-CII tube. Maximum heat transfer increases of 40% compared to CFC-114 and 30% compared to HFC-236ea were obtained by the 1024-fpm tube and the 1575-fpm tube, respectively. The condensation heat transfer coefficients produced by the Turbo-CII tube were similar for both HFC-236fa and HFC-236ea. Data were not taken on the Turbo-CII tube with CFC-114.

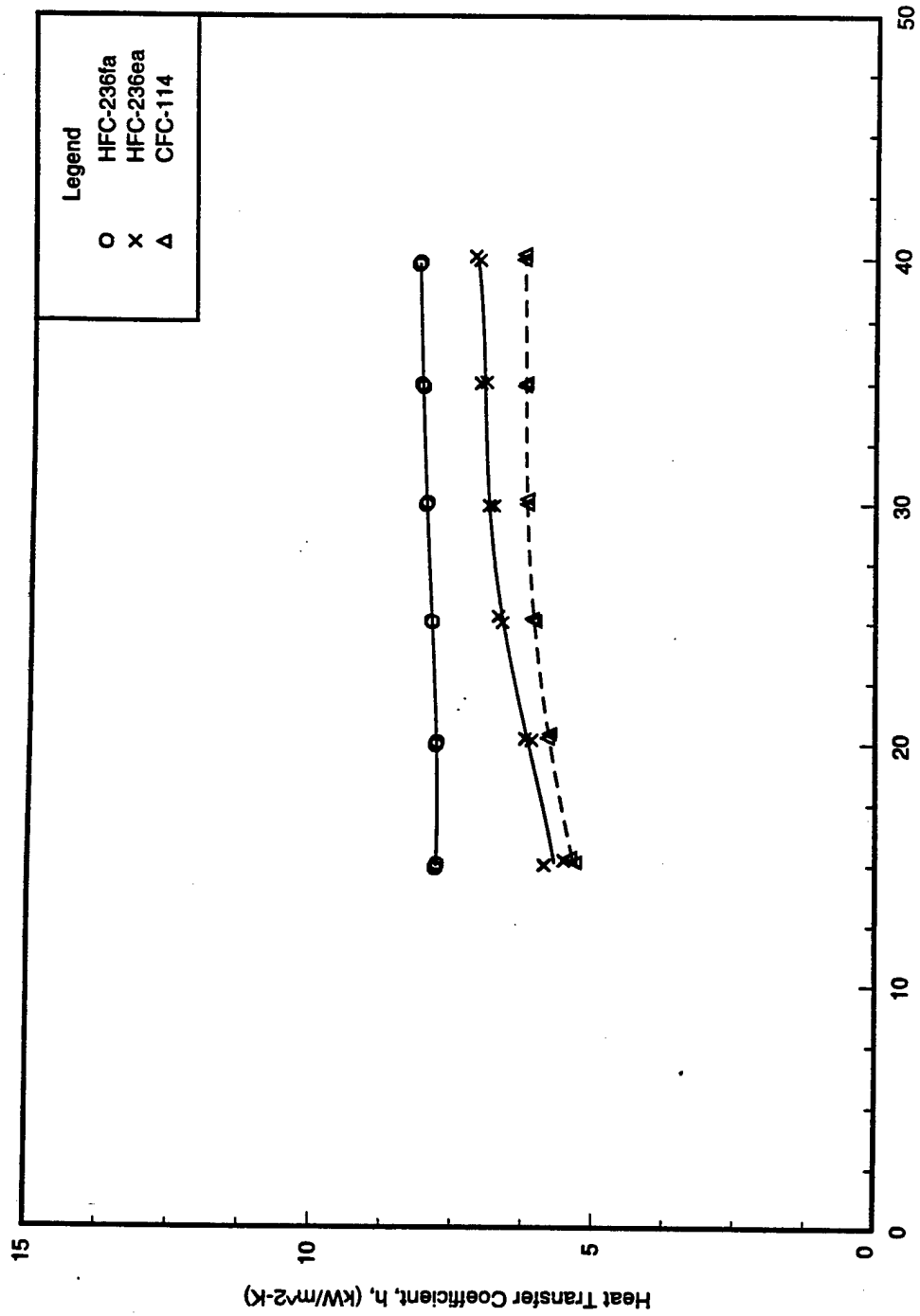

Figure 5.5. Condensation heat transfer coefficients for HFC-236fa, HFC-236ea, and CFC-114 using the 1024-fpm tube at T_{sat} = 40°C.

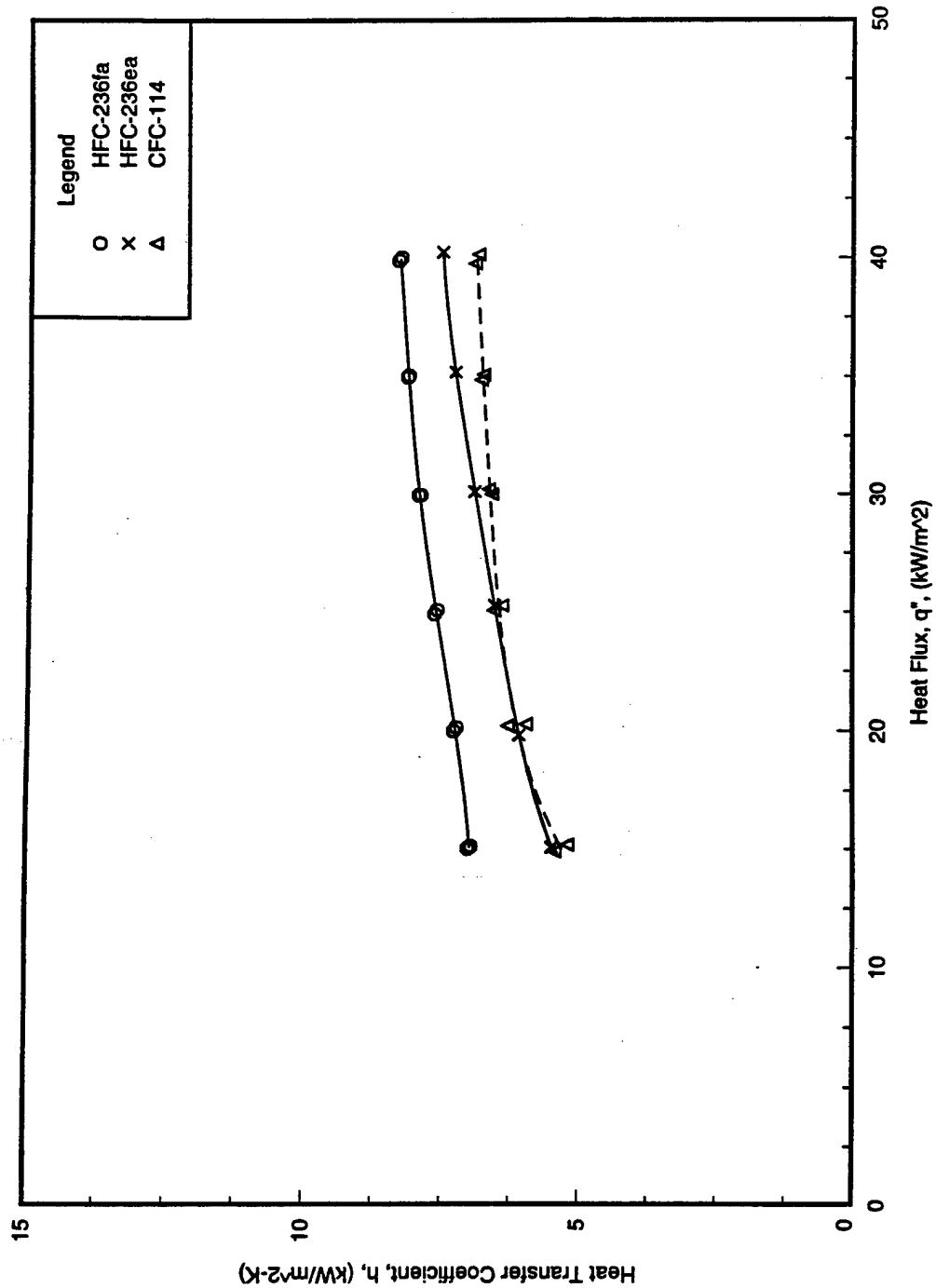

Figure 5.6. Condensation heat transfer coefficients for HFC-236fa, HFC-236ea, and CFC-114 using the 1575-fpm tube at T_{sat} = 40°C.

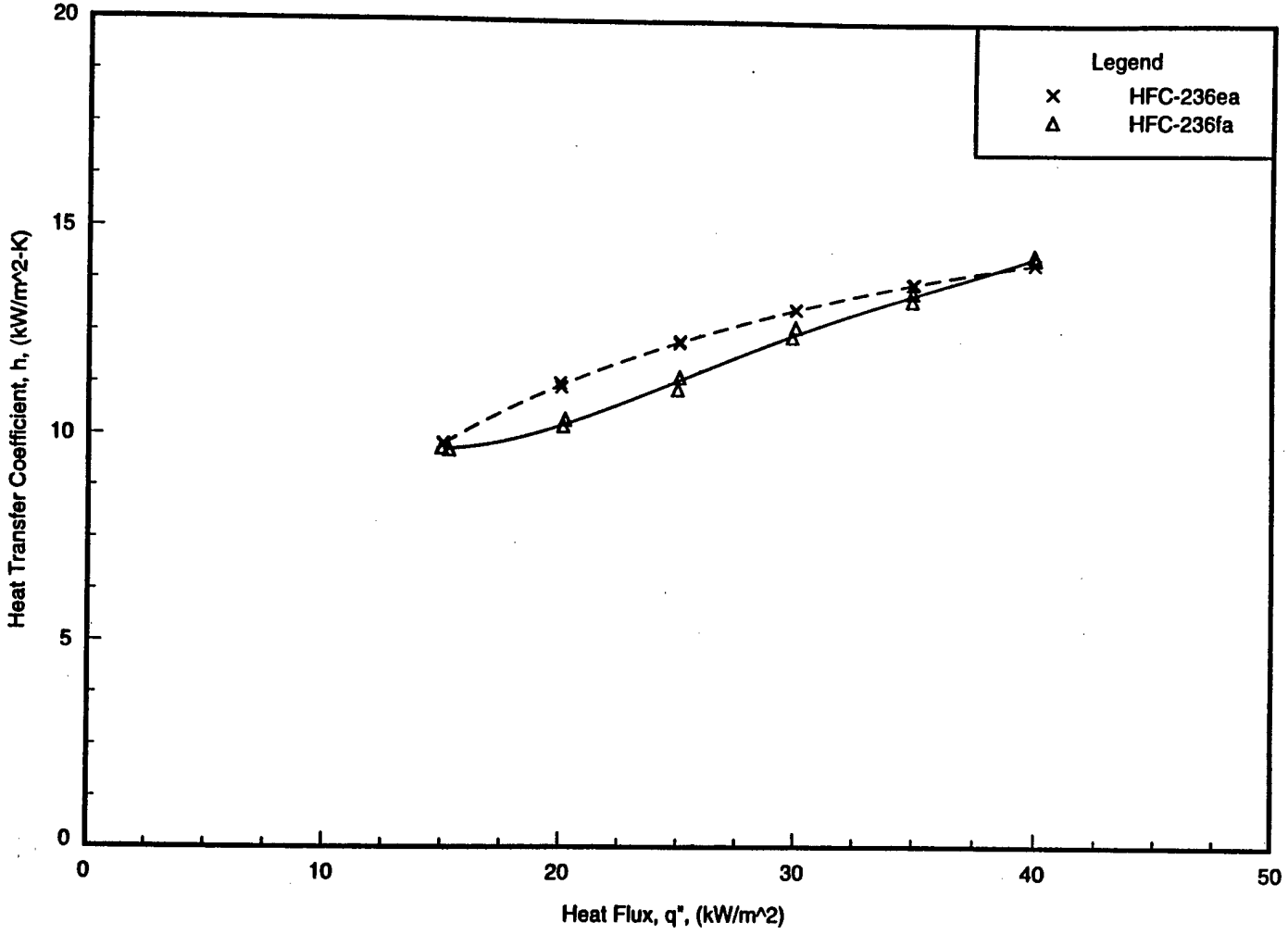

Figure 5.7. Condensation heat transfer coefficients for HFC-236ea and HFC-236fa using the Turbo-CII tube at T_{sat} = 40°C.

CHAPTER 6

POOL BOILING RESULTS

OVERVIEW

Boiling is vaporization of liquid that occurs at the interface of a solid and liquid as the temperature of the heated surface exceeds the saturation temperature of the liquid. Pool boiling is boiling from a heated surface immersed in a pool of stationary liquid. During pool boiling, the fluid motion near the heated surface is created due to free convection and bubble motion. The pool boiling curve plotted in terms of surface heat flux against wall superheat is usually used to explain pool boiling heat transfer, and it is composed of four main regimes— free convection, nucleate boiling, transition boiling, and film boiling, in ascending order of wall superheat [14].

The investigation reported here is for saturated pool boiling, where the temperature through most of the bulk liquid remains at or slightly above the saturation temperature (i.e., boiling point) and is nucleate boiling, where a certain amount of wall superheat causes vapor nucleation from the imperfections of the heating surface.

Nucleate pool boiling is a very effective mode of heat transfer because of its attractive high heat transfer rate associated with a relatively small wall superheat. However, none of the theoretical models developed or the phenomena observed satisfactorily explain the great improvement in heat transfer in this region, since the process of nucleate pool boiling combining the heat transfer mechanisms of bubble motion, thermal boundary layer stripping, and evaporation [7] is complex.

Because the shell-side boiling mechanism consists of both nucleate boiling and forced convection vaporization (convective evaporation), the heat transfer coefficient of nucleate pool boiling is required for predicting the overall shell-side heat transfer performance. However, knowledge of the mechanisms associated with nucleate boiling as well as convective evaporation on enhanced tubes is limited.

Surface roughness has been known to improve nucleate boiling performance for more than 60 years. Experimental evidence indicates that the configuration of the heated surface has definite effects on the boiling rate for either pure refrigerants or refrigerant-oil mixtures. Surfaces with a high density of re-entrant cavities that can provide stable nucleation sites require lower superheat to initiate and sustain boiling. Nevertheless, the advantage of numerous re-entrant cavities may diminish during boiling in the presence of oil since these cavities can be blocked by immiscible lubricants.

Four tubes with two distinctively different surface geometries, which were tested using HFC-236fa and HFC-236fa with oil in this research, include two integral finned tubes (1024-fpm and 1575-fpm tubes) and two high performance enhanced tubes (Turbo-B and Turbo-BII tubes). Their heat transfer performance was compared not only with each other but also with previous results for CFC-114 and HFC-236ea in the following sections.

Surface geometries were shown by the investigators to significantly affect boiling heat transfer. A number of studies concerning the boiling mechanism on different surface geometries have been published. For example, the evolution of enhanced surface geometries for nucleate boiling was surveyed by Webb [23]. A detailed discussion on enhanced boiling surfaces was provided by Thome [20]. Later, a comprehensive literature survey of 61 references involving pool boiling on enhanced surfaces was made by Pais and Webb [17]. Pais and Webb concluded that the enhanced surfaces in the existing data for refrigerants provided 2 to 4 times greater heat transfer coefficients than the integral finned tubes.

Other parameters that can affect pool boiling, such as the gravitational field and liquid subcooling, were reported to be negligible for nucleate pool boiling [14].

POOL BOILING RESULTS FOR HFC-236fa

The heat transfer data for the 1024-fpm, 1575-fpm, Turbo-B, and Turbo-BII tubes were tested and compared with each other. Results were plotted in the form of heat transfer coefficient versus heat flux in Figure 6.1 and versus excess temperature in Figure 6.2. The high performance enhanced tubes performed better during nucleate boiling than the finned tubes.

Figure 6.1 shows that the heat transfer coefficient increased as the heat flux increased for all the tubes tested. With increasing heat flux, the more violent fluid motion in the pool is induced by numerous vapor bubbles which are generated at the increased active nucleation sites and results in increased heat transfer. Figure 6.1 also shows that the two high performance enhanced tubes produced higher heat transfer coefficients at a specified heat flux than the two finned tubes.

Figure 6.2 shows the variation of heat transfer coefficient versus wall superheat for all tube types tested. The heat transfer coefficients for all the tube types tested depended on the temperature difference between the heated surface and the saturated refrigerant (i.e., excess temperature or wall superheat), and they increased as the excess temperature increased. A specified heat transfer coefficient was accomplished with a smaller wall superheat by using a high performance enhanced tube (either a Turbo-B or Turbo-BII tube) rather than an integral finned tube (either a 1024-fpm or 1575-fpm tube). Specifically, the Turbo-BII tube required the smallest wall superheat to obtain the same heat transfer rate. In other words, the Turbo-BII tube resulted in the largest heat transfer coefficient at the same wall superheat.

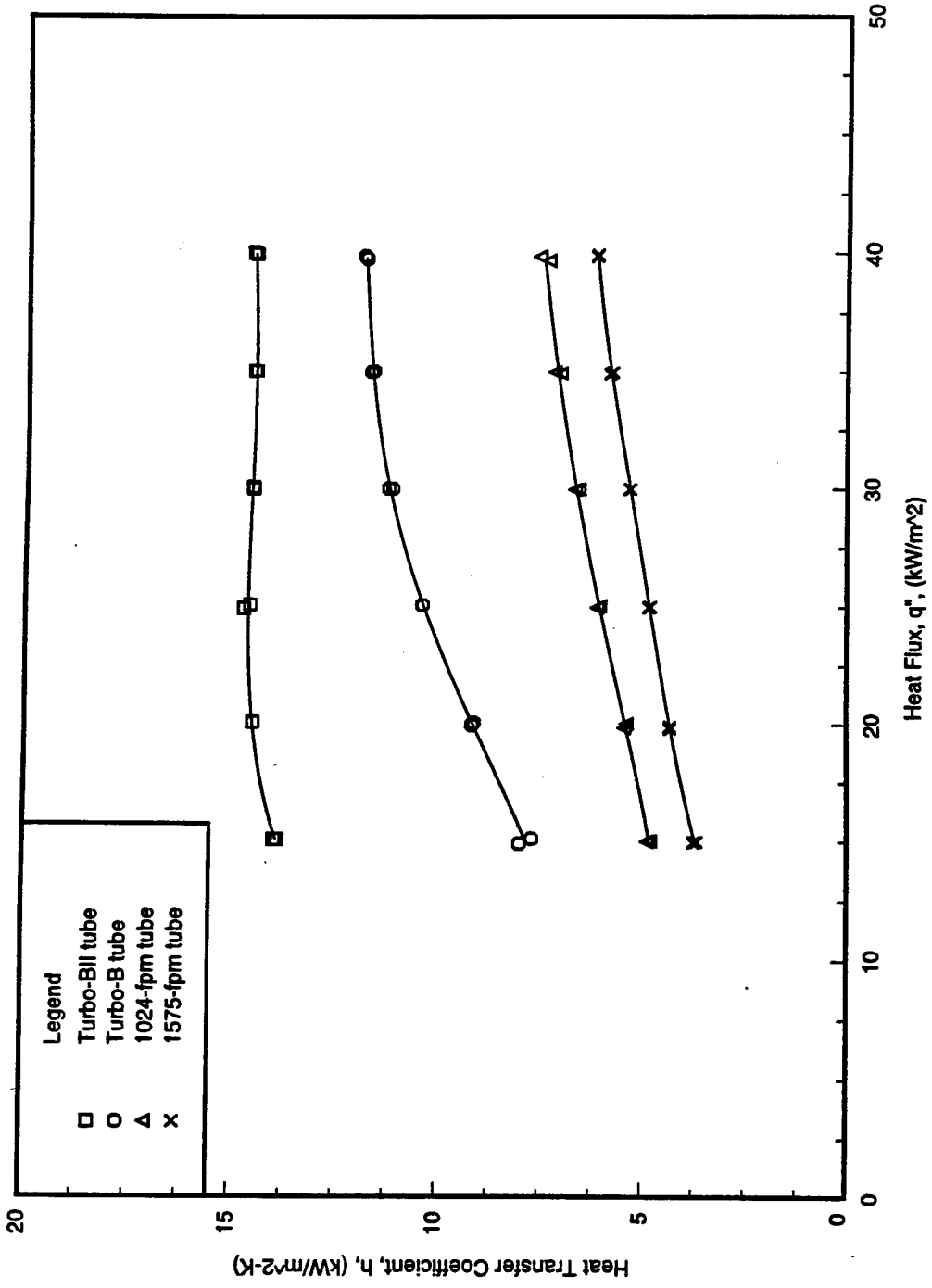

Figure 6.1. Heat transfer coefficients for HFC-236fa using the Turbo-BII, Turbo-B, 1024-fpm, and 1575-fpm tubes in pool boiling at T_{sat} = 2°C.

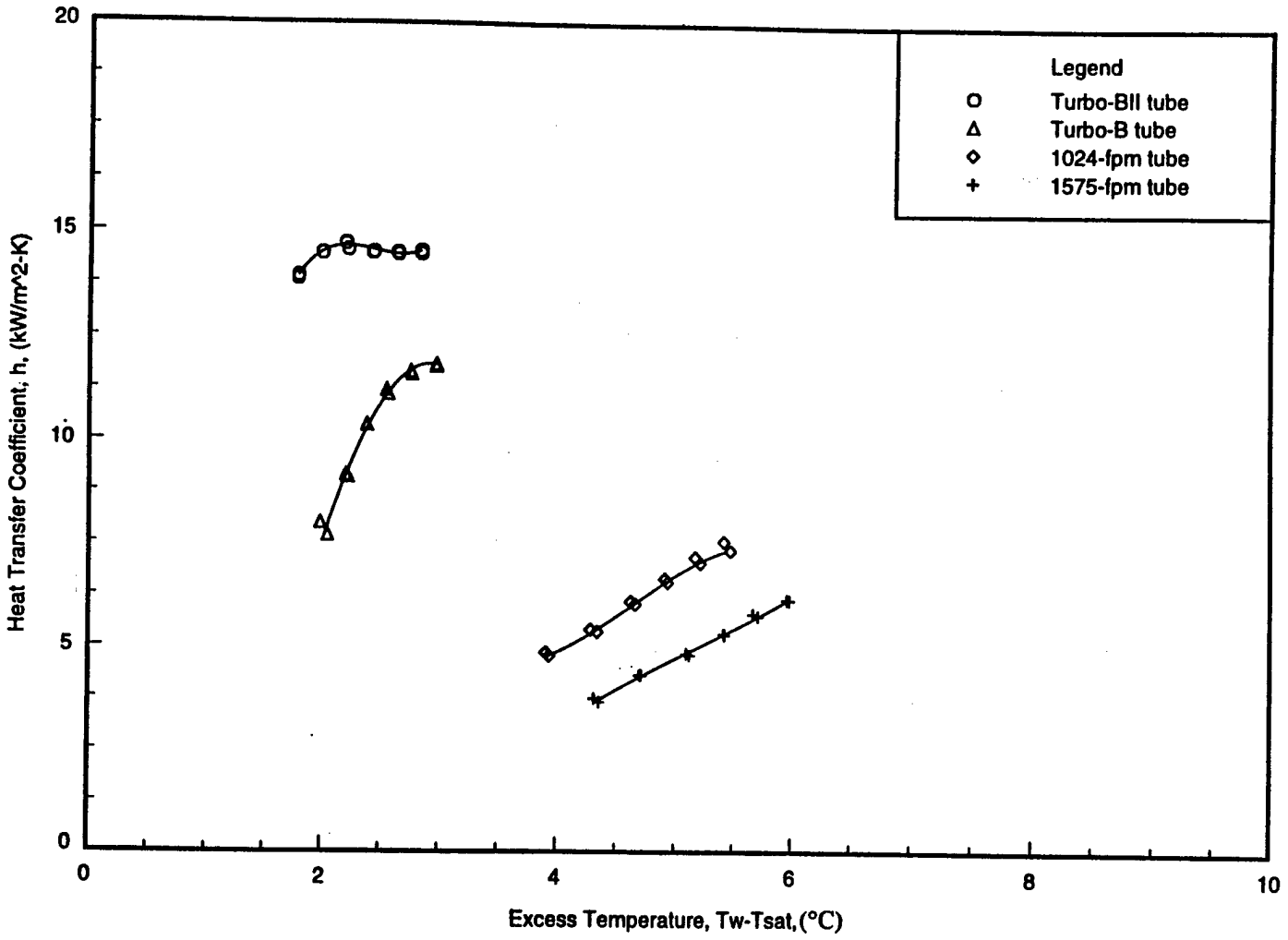

Figure 6.2. Excess temperature effects on heat transfer coefficients for HFC-236fa in pool boiling at T_{sat} = 2°C.

The Turbo-B tube yielded approximately 1.6 to 1.7 times the heat transfer coefficients of the 1024-fpm tube and 1.9 to 2.2 times the values of the 1575-fpm tube. The heat transfer performance produced by the Turbo-BII tube was around 2.0 to 2.9, 2.4 to 3.8, and 1.2 to 1.8 times as large as the values given by the 1024-fpm tube, 1575-fpm tube, and Turbo-B tube, respectively.

Webb and Pais [27] presented pool-boiling data on three tube types in a single-tube test section. The Turbo-B tube was founded to provide 1.35 and 1.3 times the performance of the 1024-fpm tube for HCFC-123 and HFC-134a, respectively.

All the experiments for pool boiling performed here were in order of decreasing heat flux to avoid hysteresis effects. The repeatability of the experiments can be seen in Figures 6.1 and 6.2.

COMPARISON OF RESULTS FOR CFC-114, HFC-236ea, AND HFC-236fa

Figures 6.3 through 6.6 clarify the effects of refrigerant types (CFC-114, HFC-236ea, and HFC-236fa) on pool boiling heat transfer. The heat transfer results for all the tubes tested show that the three different refrigerants had similar trends, with the order of descending heat transfer coefficients being: HFC-236fa, HFC-236ea, and CFC-114.

The increase in heat transfer coefficients for pool boiling with HFC-236fa compared to CFC-114 was around 50% to 80% for the 1024-fpm tube and 40% to 70% for the 1575-fpm tube. When compared to HFC-236ea, the HFC-236fa performance was about 10% to 20% higher for the 1024-fpm tube, 10% for the 1575-fpm tube, 40% to 60% for the Turbo-B tube, and 40% to 70% for the Turbo-BII tube.

POOL BOILING RESULTS FOR HFC-236fa/OIL MIXTURES

Saturated pool boiling of HFC-236fa on a single horizontal tube in the presence of oil was investigated. A miscible polyol-ester oil was added to HFC-236fa with oil concentrations of 1% and 3% by weight in order to assess the effects of the oil on the boiling performance. The polyol-ester oil used in this study has a viscosity of 340 SSU* at 37.8°C (100°F) and the trade name of Castrol Icematic SW-68.

Figures 6.7 through 6.10 show that the variation of the heat transfer coefficient with heat flux at three oil concentrations (0%, 1%, and 3%) for the 1024-fpm tube, 1575-fpm tube, Turbo-B tube, and Turbo-BII tube, respectively. As can be seen in these figures, the boiling heat transfer coefficient depends on both the heat flux and the oil concentration.

---

* Saybolt Second Universal

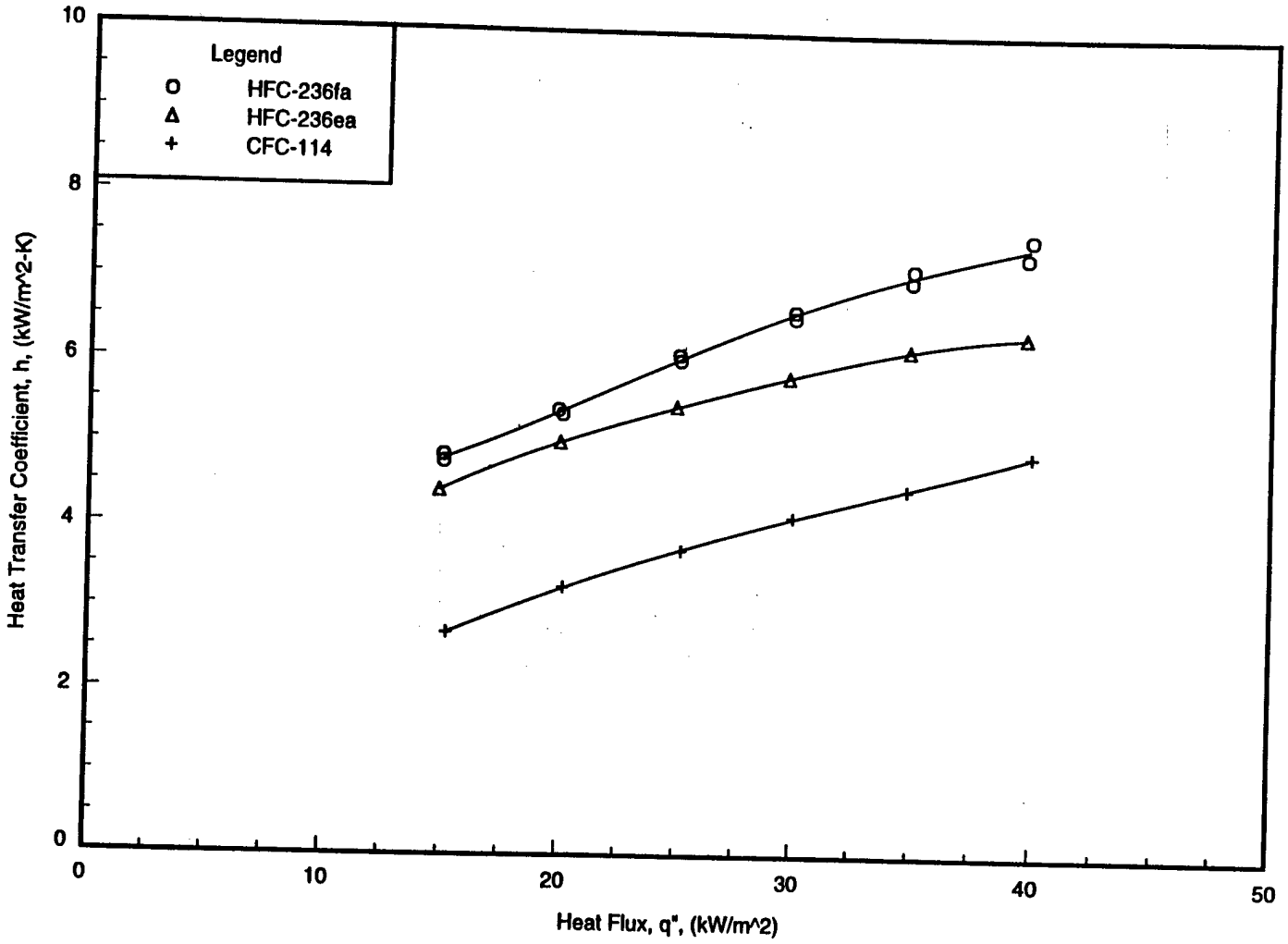

Figure 6.3. Heat transfer coefficients for HFC-236fa, HFC-236ea, and CFC-114 using the 1024-fpm tube in pool boiling at T_{sat} = 2°C.

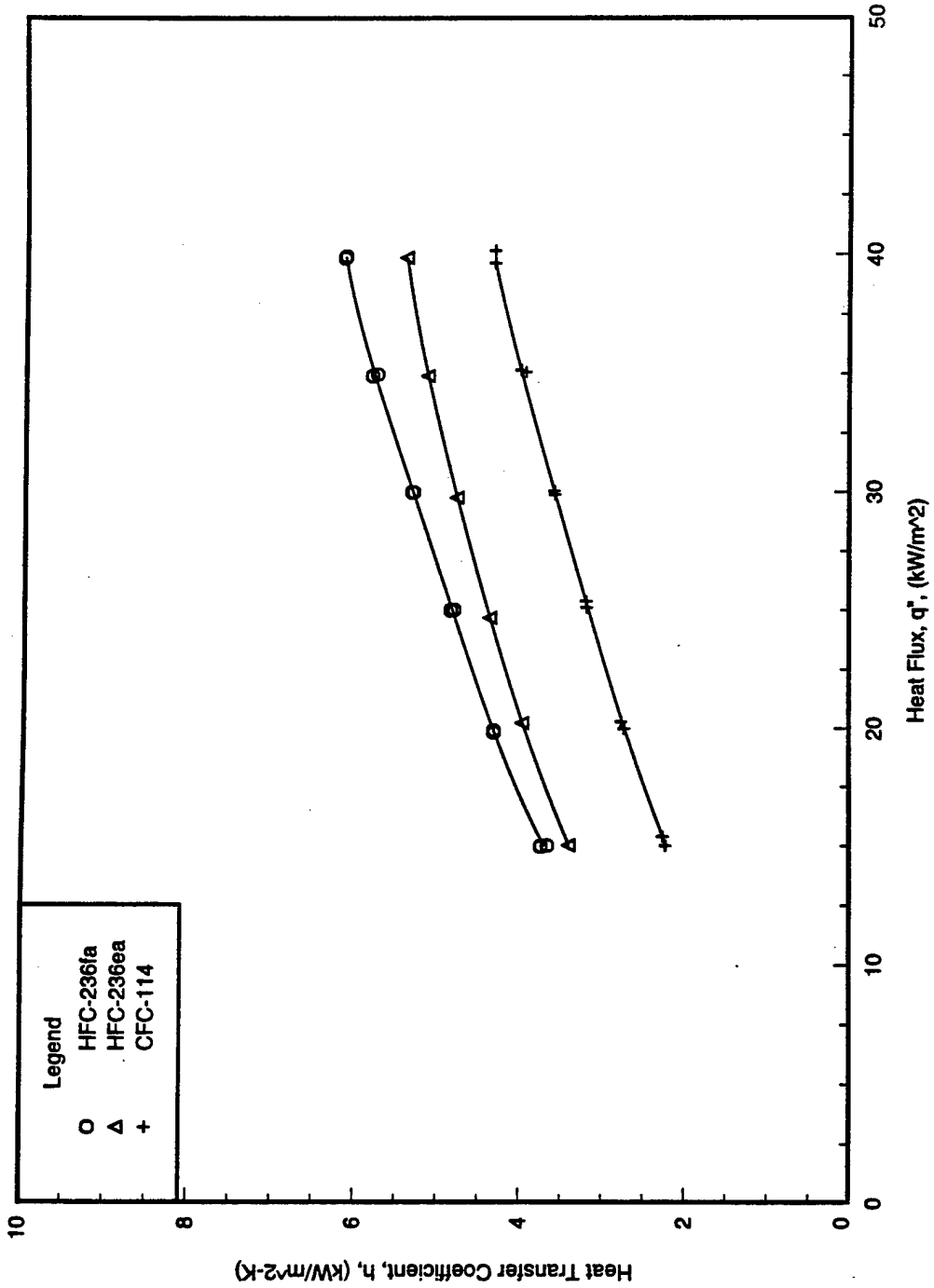

Figure 6.4. Heat transfer coefficients for HFC-236fa, HFC-236ea, and CFC-114 using the 1575-fpm tube in pool boiling at T_{sat} = 2°C.

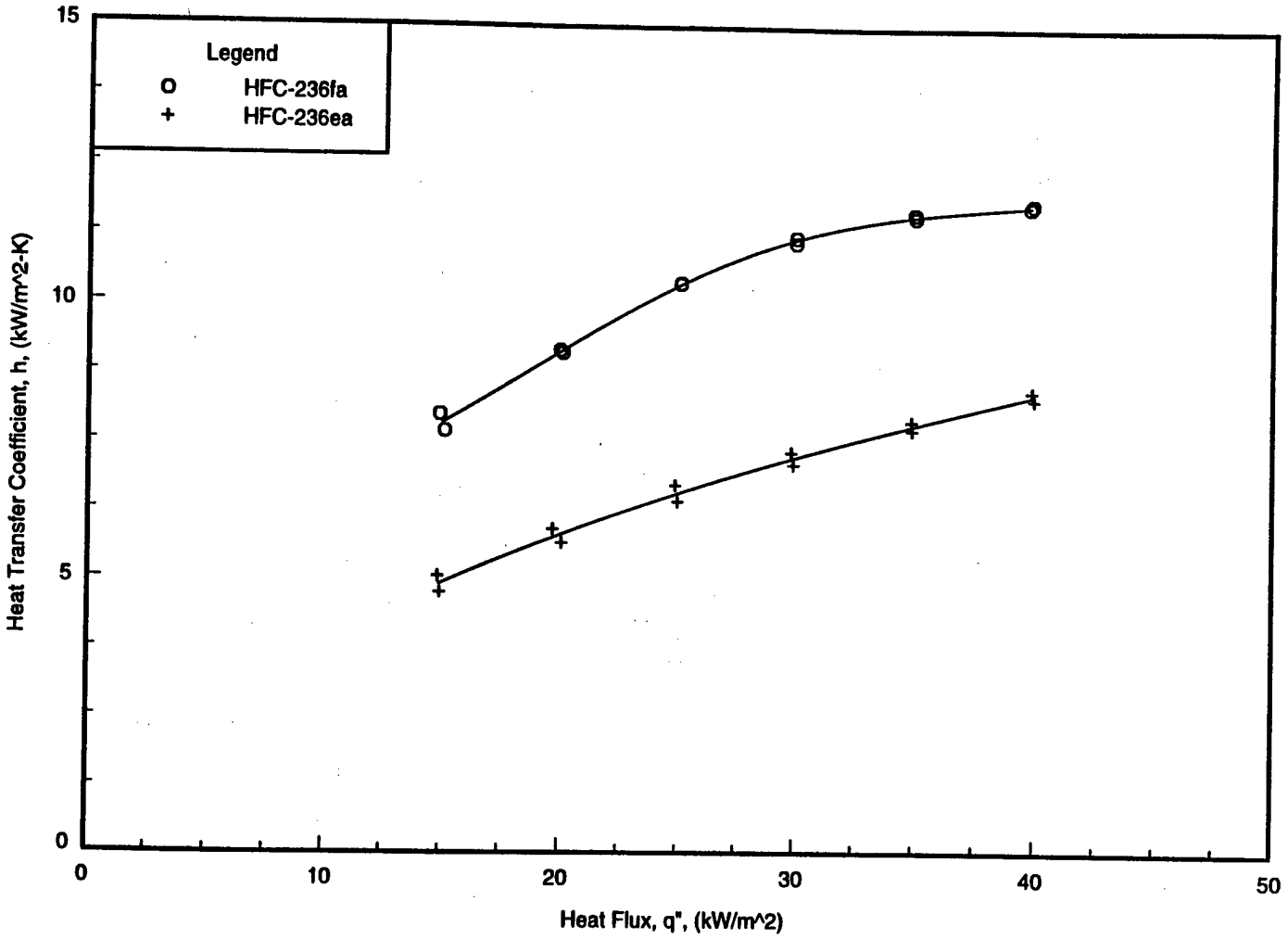

Figure 6.5. Heat transfer coefficients for HFC-236fa and HFC-236ea using the Turbo-B tube in pool boiling at T_{sat} = 2°C.

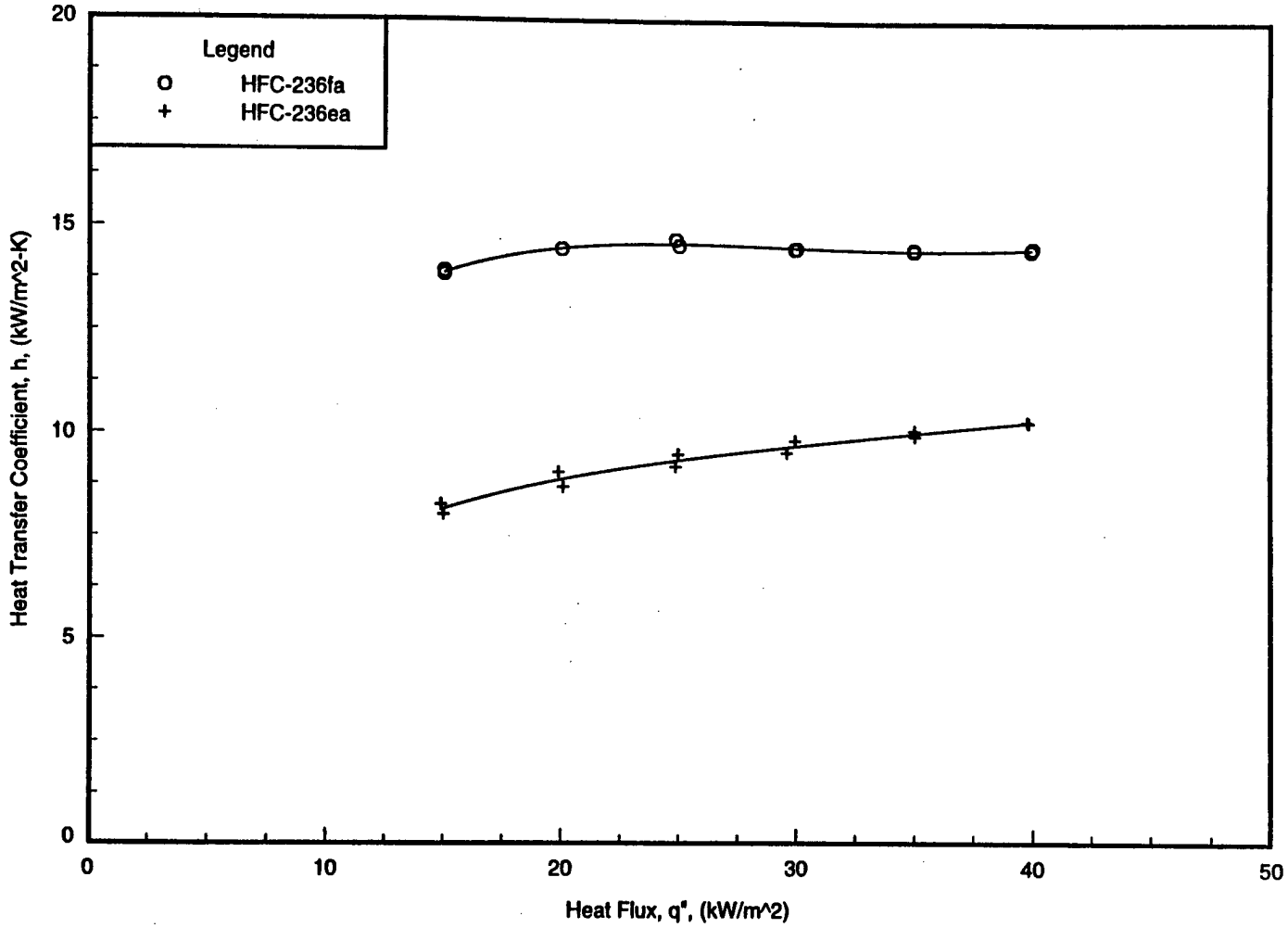

Figure 6.6. Heat transfer coefficients for HFC-236fa and HFC-236ea using the Turbo-BII tube in pool boiling at T_{sat} = 2°C.

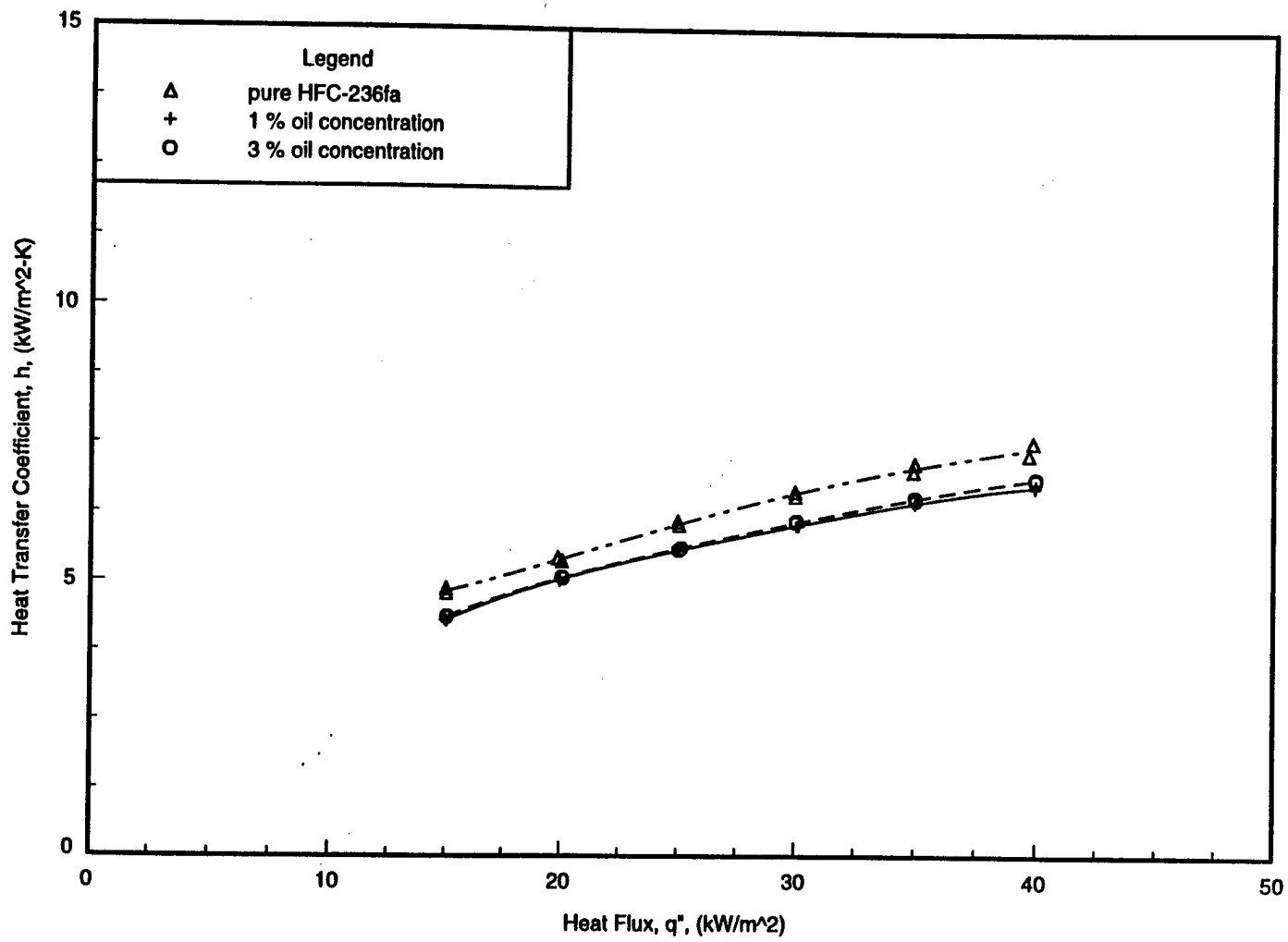

Figure 6.7. Oil effects on heat transfer coefficients of HFC-236fa using the 1024-fpm tube in pool boiling at T_{sat} = 2°C.

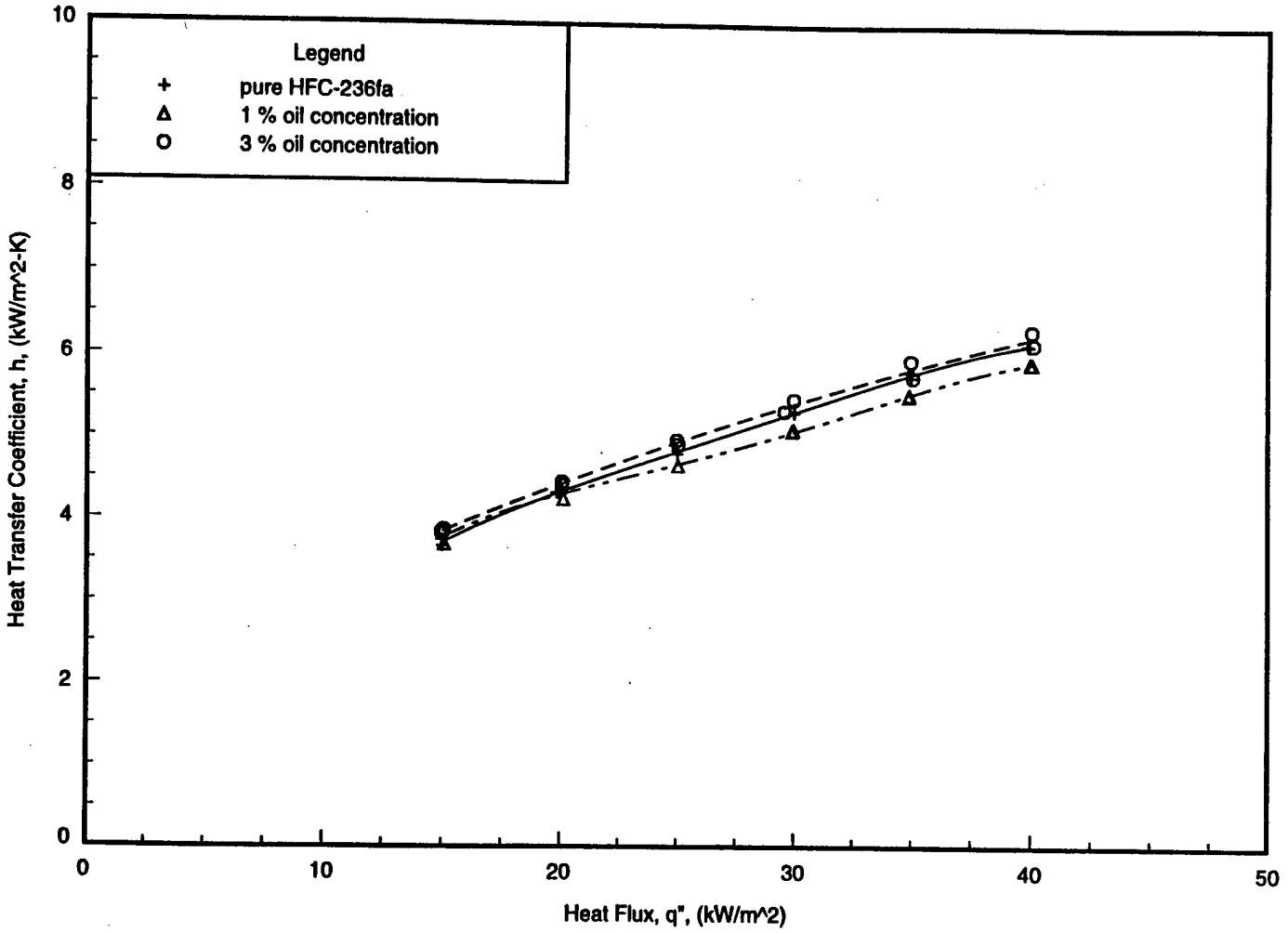

Figure 6.8. Oil effects on heat transfer coefficients of HFC-236fa using the 1575-fpm tube in pool boiling at T_{sat} = 2°C.

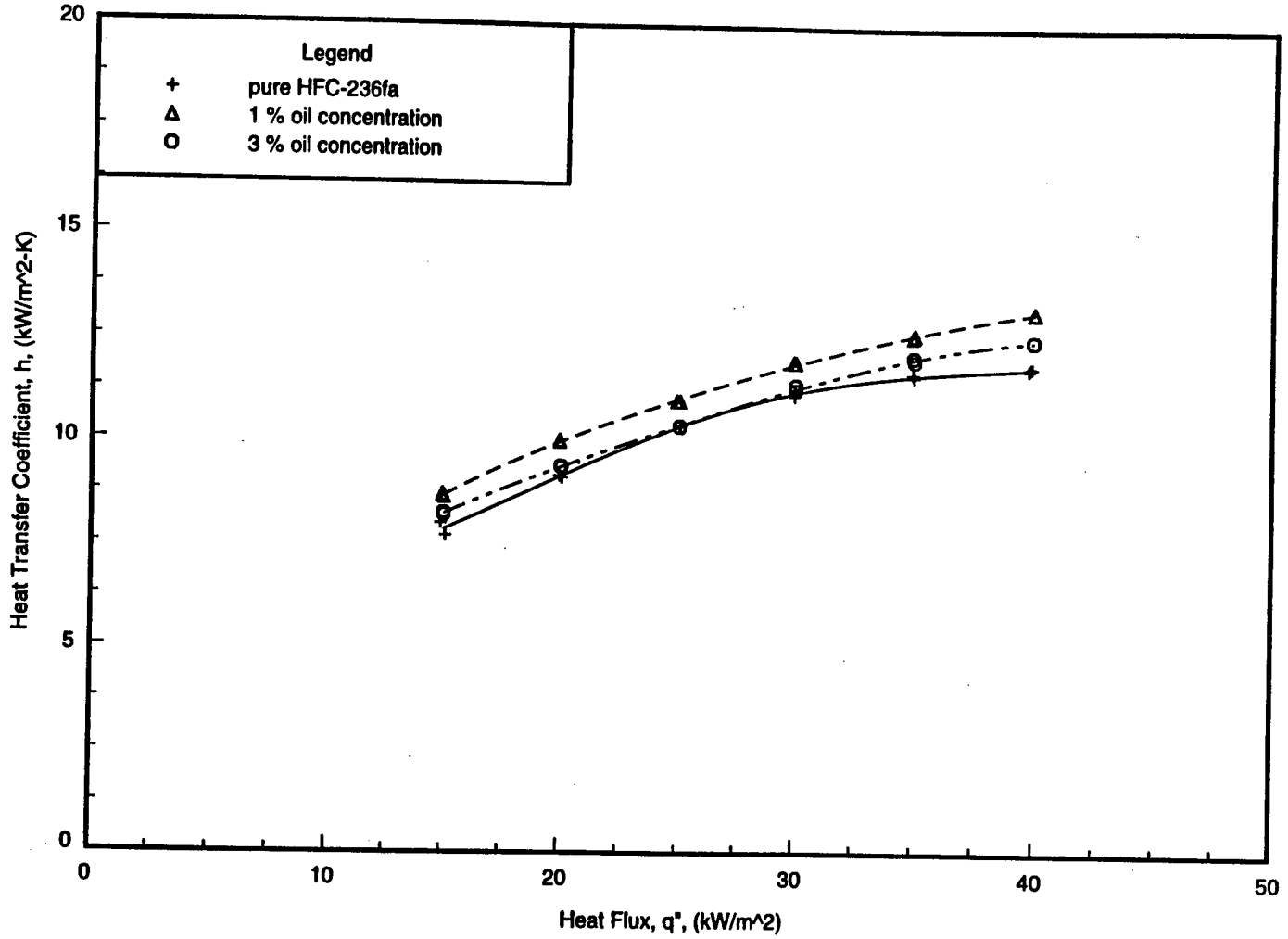

Figure 6.9. Oil effects on heat transfer coefficients of HFC-236fa using the Turbo-B tube in pool boiling at T_{sat} = 2°C.

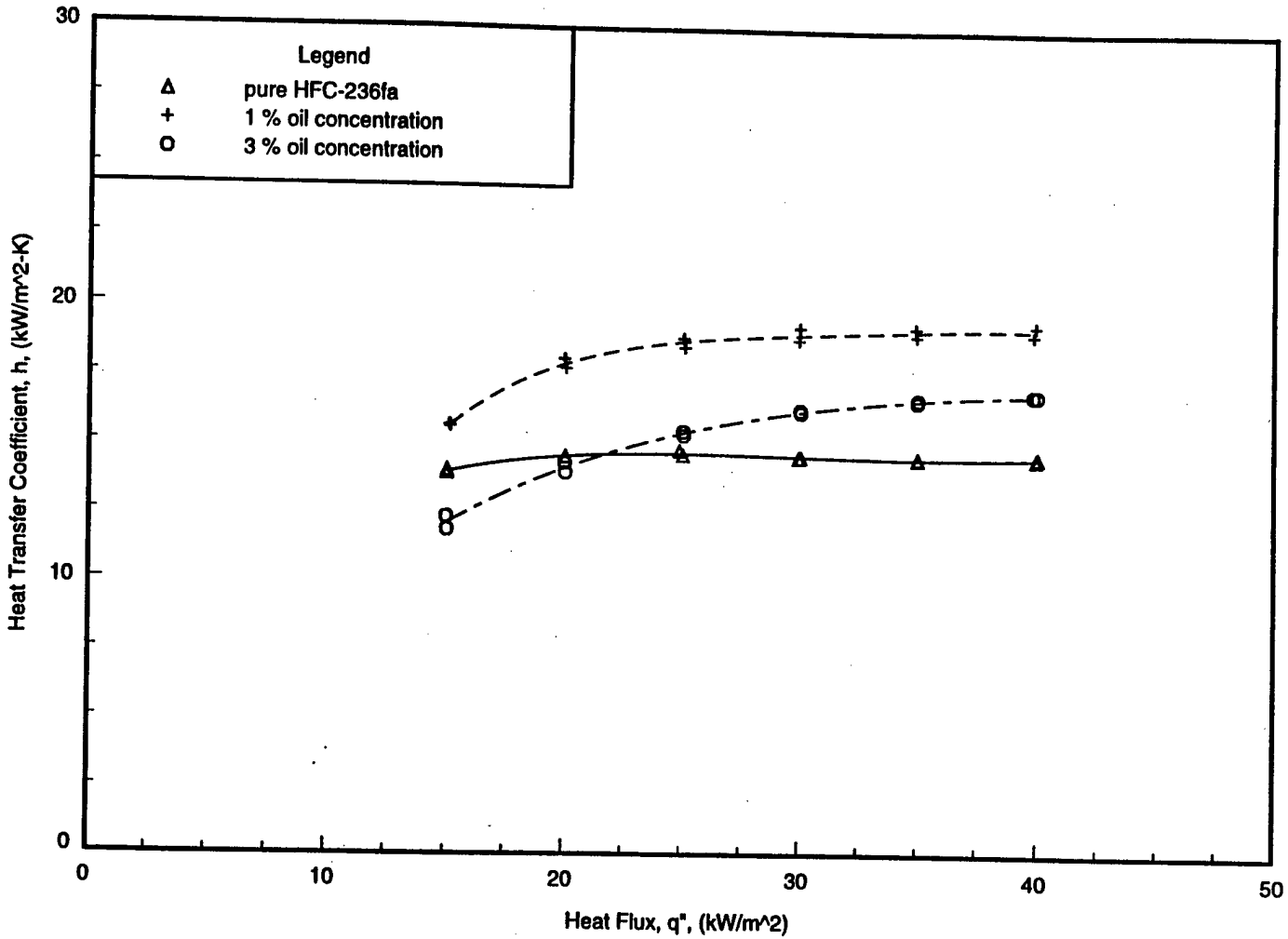

Figure 6.10. Oil effects on heat transfer coefficients of HFC-236fa using the Turbo-BII tube in pool boiling at T_{sat} = 2°C.

It is difficult to summarize a systematic dependence of each tube on the oil concentration since the polyol-ester oil used with HFC-236fa caused insignificant change in the heat transfer performance of most tubes, and most of the change was within the experimental uncertainty. The small amount of oil, up to 3% concentration, present during pool boiling was found to affect the heat transfer performance by less than 10% compared with the pure HFC-236fa for all but one of the tubes tested. The exception was the Turbo-BII tube. As noted, the Turbo-BII tube showed the largest increase in heat transfer performance with a 30% increase at 1% oil and a 15% enhancement at 3% oil over the pure refrigerant value.

In general, the heat transfer coefficients for HFC-236fa with 1% oil relative to those for pure HFC-236fa decreased for the two finned tubes, but increased for the two high performance enhanced tubes. In comparison with the 1% oil case, the heat transfer coefficients with 3% oil concentration increased for the two finned tubes, but decreased for the two high performance enhanced tubes.

As shown in Figure 6.7, the addition of oil decreased the heat transfer coefficients for the 1024-fpm tube up to 10% at both concentrations tested relative to the oil-free refrigerant. The 1024-fpm tube exhibited identical performance for pool boiling of HFC-236fa at the two oil concentrations.

Figure 6.8 shows that the small amount of oil (1% and 3%) in HFC-236fa caused the boiling coefficients for the 1575-fpm tube to differ by less than 5% from the pure refrigerant's boiling coefficients. Since the small deviation in the heat transfer coefficients caused by the addition of oil was within the experimental uncertainty, the presence of oil in refrigerant had almost no effect on heat transfer.

Memory et al. [15] reported the presence of alkylbenzene oil in HCFC-124 had a negligible effect on the boiling performance of the 1024-fpm tube over the whole oil concentration range tested (0% ~ 10%) in their tests of 748-fpm, 1024-fpm, Turbo-B, and High-Flux tubes at 2.2°C. Generally, the heat transfer performance of the smooth and finned tubes increased with increased oil concentration up to 6% and decreased with further oil addition. The heat transfer increase at 6% oil was by up to 22% and 16% for the smooth tube and the 748-fpm tube, respectively. The authors attributed this increase to the foaming that occurred. Even though the performance of the High Flux and Turbo-B tubes decreased with any increase in oil concentration and dropped by 18% and 35% at 10% oil, respectively, the two tubes had the highest heat transfer coefficients at practical design heat fluxes (10~30 kW/m^2) and oil concentration (3%).

Compared with pure HFC-236fa, the heat transfer performance of the Turbo-B tube shown in Figure 6.9 was improved by up to 10% at the 1% oil concentration but only up to 5% at the 3% oil concentration.

As shown in Figure 6.10, the heat transfer coefficients of HFC-236fa with a 1% oil concentration for the Turbo-BII tube were 10% to 30% higher than those of the pure HFC-236fa. With a 3% oil concentration, they fell below those of pure HFC-236fa over about the lowest third of heat fluxes, but were greater than the pure coefficients over the remaining range of higher heat fluxes. Specifically, the heat transfer coefficients in the case of 3% oil were 10% lower compared to pure HFC-236fa at the lowest heat flux of 15 kW/m^2, but gradually increased and finally were 15% greater at the highest heat flux of 40 kW/m^2. The coefficients for both oil

concentrations were approximately equal at 22 kW/m^2. The reason for the degradation with 3% oil at lower heat fluxes may be due to the filling of surface cavities with oil associated with the less vigorous boiling where the thermal diffusion of the heavier oil component is slow.

The differences in the surface geometries between finned tubes and high performance enhanced tubes can result in different heat transfer behaviors in the mixtures of HFC-236fa and oil. For example, the effects of oil can be more pronounced on a high performance enhanced surface than on a finned surface, since the numerous re-entrant cavities provided on the boiling surface of the high performance enhanced tubes tend to trap more oil locally than in the bulk mixture. Webb and McQuade [25] reported a larger performance degradation of enhanced tubes compared to a plain tube in mixtures of refrigerant and oil.

Pool boiling of CFC-11 and HCFC-123 with the oil concentration varying from 0% to 5% on a horizontal plain tube and two enhanced tubes (W-SE and Turbo-B tubes) was investigated at 4.4°C by Webb and McQuade [25]. Their data show that the boiling coefficients for all the geometries decreased with increased content of the mineral oil, and a larger performance degradation occurred for the enhanced tubes than for the plain tube. For 5% oil, the heat transfer performance of the plain tube, W-SE tube, and Turbo-B tube decreased by 15%, 24%, and 28%, respectively. Furthermore, the oil degraded the boiling performance of CFC-11 more than that of HCFC-123. At 2% oil, the performance degradation for the enhanced tubes was found to be 10% for HCFC-123 and 20% for CFC-11. As also reported by Memory et al. [15], the Turbo-B tube exhibited the largest adverse effect of oil.

While a number of experimental studies that deal with lubricating oil's effects on nucleate boiling coefficients have been performed, the phenomena observed on boiling of oil and refrigerant mixtures have yet to be understood completely and explained satisfactorily.

The thermophysical properties of the pool liquid during boiling (specifically, the surface tension, viscosity, and vapor pressure) change due to the addition of oil to pure refrigerant. Therefore, the wall superheat necessary to initiate vapor bubbles, the size of bubbles, the frequency of bubbles' departure from the heating surface, and the heat transfer rate change as these properties change.

Boiling of the oil and refrigerant mixtures is dominated by the combined processes of heat and mass transfer. The mixtures of oil and refrigerant are binary mixtures. Binary mixtures usually have lower evaporation rates than single-component fluids because of their low interfacial mass transfer rates. The viscous oil-rich film built up at the vapor-liquid interface reduces bubble growth rate and contributes to the decreased heat transfer performance. Some experiments [22], [24], [25] confirmed that the additional oil decreases heat transfer. However, a number of studies indicated that heat transfer coefficients increased when refrigerant was mixed with a small amount of oil, which was attributed by some researchers to the foaming activity occurring at the phase interface [13], [15].

The effects of oil on the heat transfer performance of CFC-114 with up to 10% oil (by mass) during pool boiling on a porous-coated tube and on a smooth tube were investigated at −2.2°C and 6.7°C by Wanniarachchi et al. [22]. They reported that the presence of up to 3% oil caused about a 35% reduction in the heat transfer

coefficients for the porous-coated tube over the heat flux range of 0.5 kW/m^2 to 95 kW/m^2, and the boiling performance degraded dramatically beyond the heat flux of 30 kW/m^2 with 6% or more oil. The effects of the two boiling temperatures tested were found to be insignificant.

Wanniarachchi et al. also plotted the ratio of the heat transfer coefficient with and without oil versus oil percentage with the heat flux as a parameter to show the oil effects clearly. The heat transfer ratio for the smooth tube exhibited an inexplicable wavy pattern, while for the porous-coated tube it always decreased as the oil percentage increased.

Measurements of heat transfer coefficients during pool boiling of CFC-114 and HFC-236ea with oil concentrations of 0%, 1%, and 3% were conducted on a plain, 1024-fpm, and 1575-fpm tube by Huebsch and Pate [13]. The oil used was a mineral oil for CFC-114 and a polyol-ester oil for HFC-236ea. With the presence of oil in the refrigerant, Huebsch and Pate concluded that a general improvement in the heat transfer coefficients of CFC-114 resulted in contrast to the reduced coefficients of HFC-236ea. The addition of oil increased the CFC-114 coefficients up to 30% and degraded the HFC-236ea coefficients up to 17%.

The results of Huebsch and Pate show that the heat transfer performance in pool boiling depended on not only the types of refrigerants and oils but also the tube types and oil quantity present. The two finned tubes had similar heat transfer performance at both oil concentrations with CFC-114, and their performance improved by around 30% with respect to the pure CFC-114. In the case of HFC-236ea, the 1% and 3% oil concentrations decreased the heat transfer coefficients for the 1024-fpm tube by 6% and 17%, respectively. The 1575-fpm tube showed negligible oil effects on heat transfer at the 1% oil concentration, while the presence of oil produced a 10% degradation from the pure HFC-236ea results at the 3% oil concentration.

Webb et al. [24] tested HCFC-123 with a mineral oil for GEWA-SE, Turbo-B, porous surface, and plain tubes at 4.4°C. The test range for oil concentration was from 0% to 10%. Webb et al. found that the heat transfer coefficients for all the tubes with oil concentrations lower than 2% decreased but not significantly at any heat flux and concluded that effects of the small amount of oil can be neglected for all the tubes. In addition, they also reported that the mineral oil used with HCFC-123 decreased the heat transfer performance of the GEWA-SE and Turbo-B tubes more than that of the plain and porous surface tubes.

Overall, the studies reviewed above revealed that there were no significant effects of oil addition to the refrigerant on the boiling heat transfer performance for oil concentrations typically lower than 3%. A small amount of oil present was found to cause monotonic heat transfer degradation [22], [24], [25] or both heat transfer degradation and enhancement [13], [15], depending on the combined effects of tubes, refrigerants, and oils. No significant change in heat transfer performance due to oil concentrations up to 3% was also observed in this research, which agrees with the general consensus among these previous studies.

The effects of tube types on heat transfer coefficients were clarified in Figure 6.11 for pool boiling of HFC-236fa with 1% oil and in Figure 6.12 for the 3% oil case. Figures 6.11 and 6.12 as well as Figure 6.1 which compared tubes for oil-free HFC-236fa in the earlier section all show that the four tubes had similar trends with the order of descending heat transfer coefficients being: Turbo-BII tube, Turbo-B tube, 1024-fpm tube, and 1575-fpm tube. The high performance enhanced tubes (Turbo-B and Turbo-BII) provided the best heat transfer for pool boiling of HFC-236fa with oil concentrations of 3% or less, this is in general agreement with the results of Memory et al. [15].

SUMMARY

Heat transfer coefficients on four tube types (1024-fpm, 1575-fpm, Turbo-B, and Turbo-BII tubes) were determined for pool boiling of HFC-236fa as well as HFC-236fa/oil mixtures. The effects of oil and tube types on the boiling heat transfer performance were assessed. In addition, comparison was also made for the tubes tested with the results of tests on CFC-114 and HFC-236ea in order to evaluate the effects of refrigerant types on boiling performance.

The best pool boiling heat transfer performance with HFC-236fa was provided by the high performance Turbo-BII tube with the heat transfer coefficients around 2~2.9, 2.4~3.8, and 1.2~1.8 times those for the 1024-fpm tube, 1575-fpm tube, and Turbo-B tube, respectively.

HFC-236fa performed better than CFC-114 and HFC-236ea during pool boiling for all the tube types tested. The heat transfer coefficients for HFC-236fa during pool boiling were up to 80% larger than those for CFC-114 and up to 70% larger than those for HFC-236ea, which were obtained by the 1024-fpm tube and Turbo-B tube, respectively, with HFC-236fa.

The presence of up to 3% oil in HFC-236fa affected the boiling performance by less than 10% from that of pure HFC-236fa for all but one of the tubes tested. The Turbo-BII tube, the only exception, showed an increase of up to 30% in boiling coefficients relative to the pure-refrigerant values for the testing with 1% oil and a variation from −10% to 15% for 3% oil. The Turbo-BII tube exhibited the largest changes in pool boiling performance with the addition of oil.

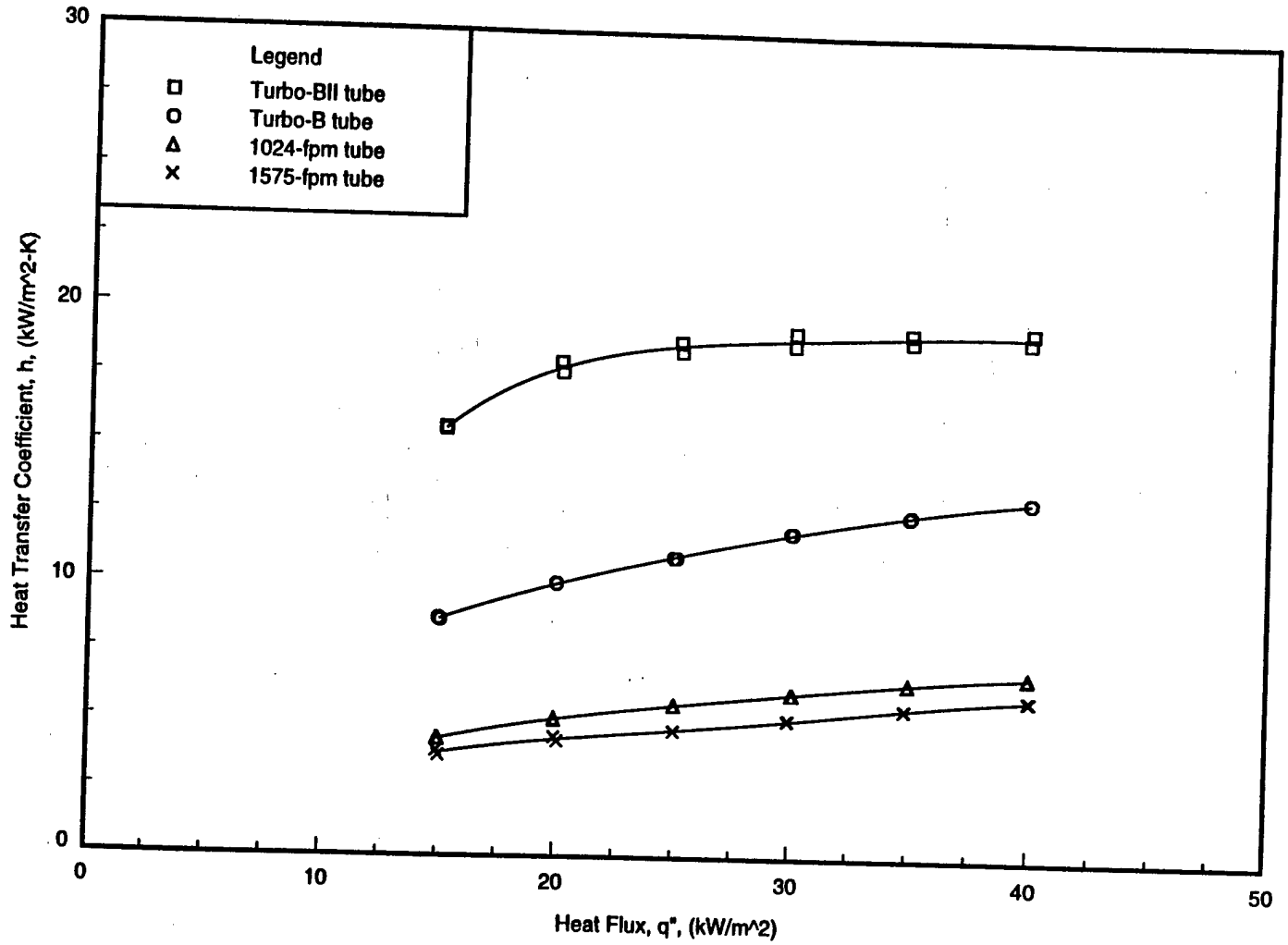

Figure 6.11. Comparison of the Turbo-BII, Turbo-B, 1024-fpm, and 1575-fpm tubes in pool boiling of HFC-236fa with 1% oil at T_{sat} = 2°C.

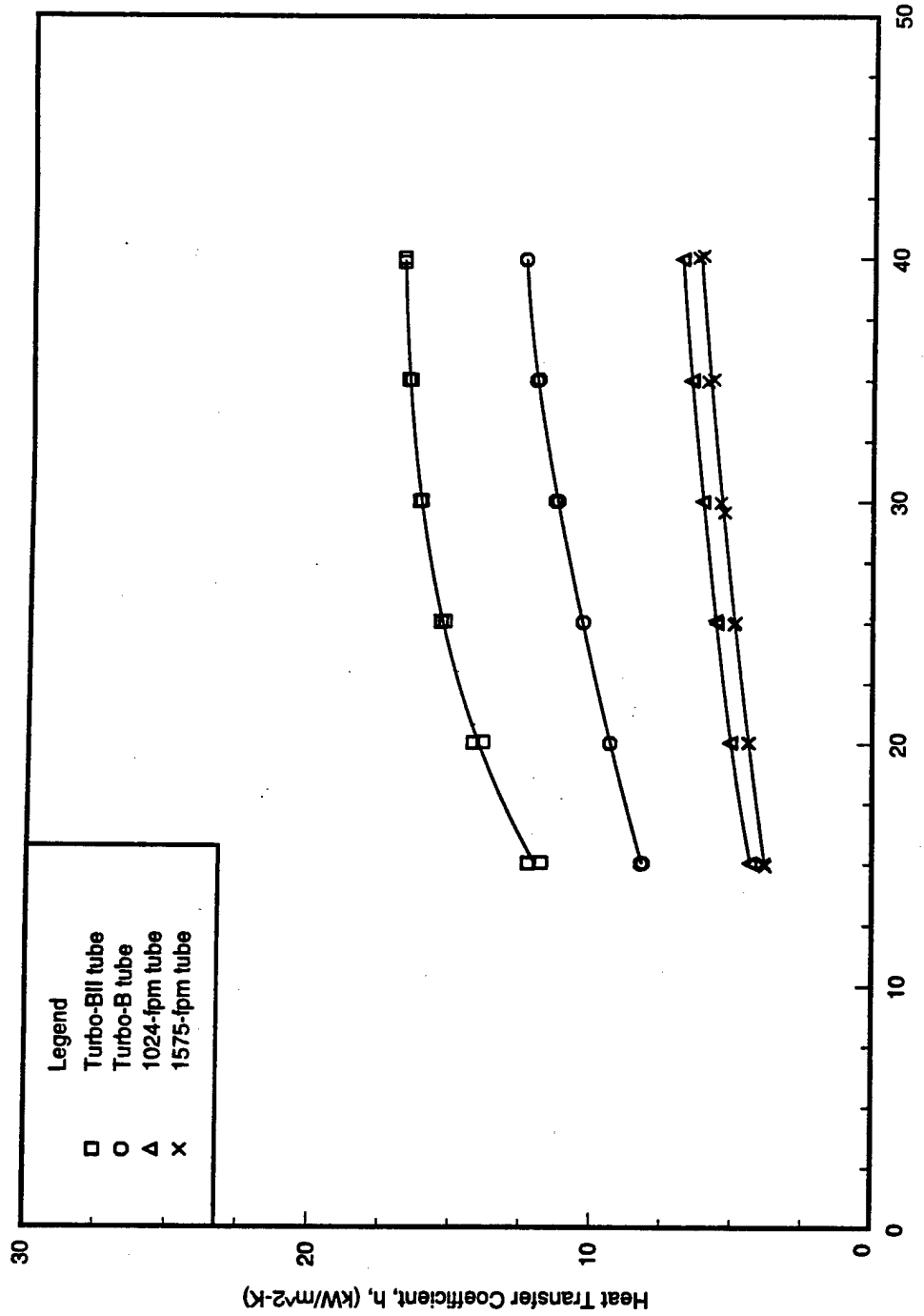

Figure 6.12. Comparison of the Turbo-BII, Turbo-B, 1024-fpm, and 1575-fpm tubes in pool boiling of HFC-236fa with 3% oil at T_{sat} = 2°C.

REFERENCES

1. Adamek, T. and Webb, R. L. 1990. "Prediction of film condensation on a horizontal integral fin tube." Int. Journal of Heat and Mass Transfer, Vol. 33, pp. 1721-1735.
2. Bella, B., Cavallini, A., Longo, G. A., and Rossetto, L. 1993. "Pure vapour condensation of refrigerants 11 and 113 on a horizontal integral finned tube at high vapour velocity." Journal of Enhanced Heat Transfer, Vol. 1, pp. 77-86.
3. Briggs, A., Baichoo, S., and Rose, J. W. 1994. "Condensation of steam and CFC113 on commercially available integral-fin tubes." Fundamentals of Phase Change: Boiling and Condensation, ASME, Heat Transfer Division, New York, NY. HTD, Vol. 273, pp. 41-47.
4. Cavallini, A., Bella, B., Longo, G. A., and Rossetto, L. 1995. "Experimental heat transfer coefficients during condensation of halogenated refrigerants on enhanced tubes." Journal of Enhanced Heat Transfer, Vol. 2, pp. 115-125.
5. Cavallini, A., Bella, B., Longo, G. A., and Rossetto, L. 1992. "Forced convection condensation on horizontal low integral fin tubes." Institution of Chemical Engineers, Rugby, England. Symposium Series, Vol. 2, No. 129, pp. 829-835.
6. Chu, C. M. and McNaught, J. M. 1992. "Condensation on bundles of plain and low-finned tubes: effect of vapor shear and condensate inundation." Institution of Chemical Engineers, Rugby, England. Symposium Series, Vol. 2, No. 129, pp. 225-229.
7. Collier, J. G. and Thome, J. R. 1994. In Chapter 4, Convective Boiling and Condensation, 3rd ed. New York: Oxford University Press, Inc.
8. Honda, H., Takamatsu, H., and Kim, K. 1994. "Condensation of CFC-11 and HCFC-123 in in-line bundles of horizontal finned tubes: effects of fin geometry." Journal of Enhanced Heat Transfer, Vol. 1, pp. 197-209.
9. Honda, H., Takamatsu, H., Takada, N., and Makishi, O. 1996. "Condensation of HCFC-123 in bundles of horizontal finned tubes: effects of fin geometry and tube arrangement." International Journal of Refrigeration, Vol. 19, pp. 1-9.
10. Huber, J. B., Rewerts, L. E., and Pate, M. B. 1994. "Shell-side condensation heat transfer of R-134a— Part I: Finned tube performance." ASHRAE Transactions, Vol. 100(2), pp. 239-247.
11. Huber, J. B., Rewerts, L. E., and Pate, M. B. 1994. "Shell-side condensation heat transfer of R-134a— Part II: Enhanced tube performance." ASHRAE Transactions, Vol. 100(2), pp. 248-256.

12. Huber, J. B., Rewerts, L. E., and Pate, M. B. 1994. "Experimental determination of shell-side condenser bundle heat transfer design factors for refrigerants R-123 and R-134a." Ph.D. Dissertation, Iowa State University.
13. Huebsch, W. W. and Pate, M. B. 1996. "Heat transfer evaluation of HFC-236ea and CFC-114 in condensation and evaporation." EPA-600/R-96-070 (NTIS PB96-183900), U. S. Environmental Protection Agency, Research Triangle Park, NC.
14. Incropera, F. P. and DeWitt, D. P. 1990. In Chapter 10, Fundamentals of Heat and Mass Transfer, 3rd ed. New York: Wiley.
15. Memory, S. B., Bertsch, G., and Marto P. J. 1993. "Pool boiling of HCFC-124/oil mixtures from smooth and enhanced tubes." Heat Transfer with Alternate Refrigerants, ASME, New York, NY. HTD, Vol. 243, pp. 9-18.
16. Murata, K. and Hashizzume, K. 1992. "Prediction of condensation heat transfer coefficient in horizontal integral-fin tube bundles." Experimental Heat Transfer, Vol. 5, pp. 115-130.
17. Pais, C. and Webb, R. L. 1991. "Literature survey of pool boiling on enhanced surfaces." ASHRAE Transactions, Vol. 97(1), pp. 79-89.
18. Rose, J. W. 1994. "An approximate equation for the vapor-side heat-transfer coefficient for condensation on low-finned tubes." Int. Journal of Heat and Mass Transfer, Vol. 37, No. 5, pp. 865-875.
19. Sukhatme, S. P., Jagadish, B. S., and Prabhakaran, P. 1990. "Film condensation of R-11 vapor on single horizontal enhanced condenser tubes." Journal of Heat Transfer, Vol. 112, pp. 229-234.
20. Thome, J. R. 1990. In Enhanced Boiling Heat Transfer, New York: Hemisphere Publishing Co.
21. Ullmann, A. and Letan, R. 1989. "Effect of noncondensibles on condensation and evaporation of bubbles." Journal of Heat Transfer, Vol. 111, pp. 1060-1067.
22. Wanniarachchi, A. S., Marto, P. J., and Reilly, J. T. 1986. "The effect of oil contamination on the nucleate pool-boiling performance of CFC-114 from a porous-coated surface." ASHRAE Transactions, Vol. 92(2B), pp. 525-538.
23. Webb, R. L. 1981. "The evolution of enhanced surface geometries for nucleate boiling." Heat Transfer Engineering, Vol. 2, pp. 46-69.
24. Webb, R. L., Chien, L.-H., McQuade, W. F., and Imadojemu, H. E. 1995. "Pool boiling of oil-refrigerant mixtures on enhanced tubes." In Proceedings: ASME/JSME Thermal Engineering Joint Conference, New York, NY. Vol. 2, pp. 247-255.
25. Webb, R. L. and McQuade, W. F. 1993. "Pool boiling of R-11 and R-123 oil-refrigerant mixtures on plain and enhanced tube geometries." ASHRAE Transactions, Vol. 99(1), pp. 1225-1236.
26. Webb, R. L. and Murawski, C. G. 1990. "Row effect for R-11 condensation on enhanced tubes." Journal of Heat Transfer, Vol. 112, pp. 768-776.
27. Webb, R. L. and Pais, C. 1991. "Pool boiling data for five refrigerants on three tube geometries." ASHRAE Transactions, Vol. 97(1), pp. 72-78.

APPENDIX A

REFRIGERANT PROPERTIES

TABLE A.1: PROPERTIES OF HFC-236fa

Temperature (°C)	Pressure (kPa)	Enthalpy (kJ/kg)	Density (kg/m^3)	Viscosity (mPa s)	Thermal Conductivity (W/m K)	Phase
2.0	117.1	204.3	8.253	10.3	0.0110	Vapor
2.0	117.1	48.6	1434.	391.9	0.0793	Liquid
40.0	436.3	229.4	29.54	12.0	0.0149	Vapor
40.0	436.3	95.2	1308.	237.9	0.0697	Liquid

APPENDIX B

GEOMETRIC SPECIFICATIONS OF TUBES

TABLE B.1 GEOMETRIC SPECIFICATIONS OF TUBES IN SI UNITS

tube	fin count (fins/m)	D_o nominal (mm)	D_i nominal (mm)	D_r (mm)	fin height (mm)	A_o/L nominal (m^2/m)	A_o/L actual (m^2/m)	A_i/L nominal (m^2/m)
1024-fpm	1024	18.8	14.4	15.9	1.45	0.0588	0.193	0.0454
1575-fpm	1575	18.8	15.7	17.1	0.86	0.0593	0.179	0.0493
Turbo-CII	N/A	18.90	15.54	17.07	0.91	0.0597	N/A	0.0488
Turbo-B	N/A	18.5	16.1	17.3	0.59	0.0582	N/A	0.0506
Turbo-BII	N/A	18.62	16.05	17.27	0.68	0.0585	N/A	0.0504

TABLE B.2 GEOMETRIC SPECIFICATIONS OF TUBES IN ENGLISH UNITS

tube	fin count (fins/in)	D_o nominal (in)	D_i nominal (in)	D_r (in)	fin height (in)	A_o/L nominal (ft^2/ft)	A_o/L actual (ft^2/ft)	A_i/L nominal (ft^2/ft)
1024-fpm	26	0.739	0.568	0.625	0.057	0.193	0.634	0.149
1575-fpm	40	0.743	0.622	0.675	0.034	0.195	0.586	0.163
Turbo-CII	N/A	0.744	0.612	0.672	0.036	0.196	N/A	0.160
Turbo-B	N/A	0.730	0.632	0.682	0.024	0.191	N/A	0.165
Turbo-BII	N/A	0.733	0.632	0.680	0.027	0.192	N/A	0.165

APPENDIX C

TABULATED DATA

The experimental data obtained in this study are presented in this appendix. Data points at six different heat fluxes were tested for each run and listed in one table.

TABLE C.1: CONDENSATION OF HFC-236fa ON THE 1024-fpm TUBE AT A SATURATION TEMPERATURE OF 40°C (PRIMARY RUN)

h (W/m^2K)	7.78E+03	7.79E+03	7.89E+03	7.99E+03	8.08E+03	8.14E+03
q" (W/m^2)	1.50E+04	2.01E+04	2.50E+04	3.00E+04	3.49E+04	3.99E+04
q (Watts)	7.54E+02	1.01E+03	1.25E+03	1.51E+03	1.75E+03	2.00E+03
LMTD (°C)	5.27E+00	6.14E+00	6.94E+00	7.71E+00	8.41E+00	9.14E+00
Δ T (°C)	2.67E+00	3.10E+00	3.49E+00	3.88E+00	4.22E+00	4.59E+00
h_i (W/m^2K)	6.05E+03	7.59E+03	8.98E+03	1.03E+04	1.16E+04	1.28E+04
Re_i	1.12E+04	1.47E+04	1.80E+04	2.13E+04	2.45E+04	2.76E+04
U_o (W/m^2K)	2.85E+03	3.26E+03	3.60E+03	3.90E+03	4.15E+03	4.36E+03
UN (± %)	8.77E+00	7.50E+00	6.80E+00	6.34E+00	6.01E+00	5.73E+00

TABLE C.2: CONDENSATION OF HFC-236fa ON THE 1024-fpm TUBE AT A SATURATION TEMPERATURE OF 40°C (REPEAT RUN)

h (W/m^2K)	7.81E+03	7.82E+03	7.91E+03	8.02E+03	8.11E+03	8.16E+03
q" (W/m^2)	1.49E+04	1.99E+04	2.51E+04	3.00E+04	3.50E+04	3.98E+04
q (Watts)	7.45E+02	1.00E+03	1.26E+03	1.50E+03	1.75E+03	2.00E+03
LMTD (°C)	5.20E+00	6.09E+00	6.95E+00	7.68E+00	8.42E+00	9.11E+00
Δ T (°C)	2.63E+00	3.07E+00	3.50E+00	3.86E+00	4.23E+00	4.57E+00
h_i (W/m^2K)	6.06E+03	7.61E+03	8.98E+03	1.03E+04	1.16E+04	1.28E+04
Re_i	1.12E+04	1.48E+04	1.80E+04	2.13E+04	2.45E+04	2.75E+04
U_o (W/m^2K)	2.85E+03	3.27E+03	3.61E+03	3.90E+03	4.15E+03	4.37E+03
UN (± %)	8.92E+00	7.55E+00	6.80E+00	6.37E+00	6.00E+00	5.75E+00

TABLE C.3: CONDENSATION OF HFC-236fa ON THE 1575-fpm TUBE AT A SATURATION TEMPERATURE OF 40°C (PRIMARY RUN)

h (W/m^2K)	7.00E+03	7.26E+03	7.62E+03	7.92E+03	8.13E+03	8.29E+03
q'' (W/m^2)	1.50E+04	2.00E+04	2.49E+04	3.00E+04	3.50E+04	3.99E+04
q (Watts)	7.53E+02	1.00E+03	1.25E+03	1.50E+03	1.75E+03	2.00E+03
LMTD (°C)	5.45E+00	6.26E+00	6.98E+00	7.69E+00	8.37E+00	9.02E+00
ΔT (°C)	2.76E+00	3.16E+00	3.51E+00	3.87E+00	4.21E+00	4.53E+00
h_i (W/m^2K)	5.65E+03	7.10E+03	8.41E+03	9.64E+03	1.08E+04	1.20E+04
Re_i	1.02E+04	1.35E+04	1.66E+04	1.95E+04	2.25E+04	2.54E+04
U_o (W/m^2K)	2.78E+03	3.22E+03	3.60E+03	3.93E+03	4.22E+03	4.47E+03
UN (± %)	8.05E+00	7.12E+00	6.61E+00	6.21E+00	5.92E+00	5.70E+00

TABLE C.4: CONDENSATION OF HFC-236fa ON THE 1575-fpm TUBE AT A SATURATION TEMPERATURE OF 40°C (REPEAT RUN)

h (W/m^2K)	6.95E+03	7.21E+03	7.58E+03	7.88E+03	8.11E+03	8.25E+03
q'' (W/m^2)	1.51E+04	2.01E+04	2.51E+04	3.00E+04	3.50E+04	4.00E+04
q (Watts)	7.58E+02	1.01E+03	1.26E+03	1.50E+03	1.76E+03	2.01E+03
LMTD (°C)	5.49E+00	6.34E+00	7.05E+00	7.70E+00	8.39E+00	9.07E+00
ΔT (°C)	2.78E+00	3.19E+00	3.55E+00	3.87E+00	4.22E+00	4.56E+00
h_i (W/m^2K)	5.67E+03	7.09E+03	8.39E+03	9.65E+03	1.08E+04	1.20E+04
Re_i	1.02E+04	1.35E+04	1.65E+04	1.95E+04	2.25E+04	2.54E+04
U_o (W/m^2K)	2.78E+03	3.21E+03	3.59E+03	3.92E+03	4.21E+03	4.45E+03
UN (± %)	7.95E+00	7.04E+00	6.54E+00	6.20E+00	5.91E+00	5.67E+00

TABLE C.5: CONDENSATION OF HFC-236fa ON THE TURBO-CII TUBE AT A SATURATION TEMPERATURE OF 40°C (PRIMARY RUN)

h (W/m^2K)	9.68E+03	1.02E+04	1.14E+04	1.26E+04	1.35E+04	1.44E+04
q'' (W/m^2)	1.50E+04	2.01E+04	2.50E+04	3.00E+04	3.50E+04	4.00E+04
q (Watts)	7.50E+02	1.01E+03	1.25E+03	1.50E+03	1.75E+03	2.01E+03
LMTD (°C)	3.02E+00	3.56E+00	3.88E+00	4.14E+00	4.42E+00	4.67E+00
ΔT (°C)	1.57E+00	1.83E+00	1.98E+00	2.11E+00	2.25E+00	2.37E+00
h_i (W/m^2K)	1.29E+04	1.62E+04	1.92E+04	2.22E+04	2.50E+04	2.78E+04
Re_i	1.08E+04	1.42E+04	1.76E+04	2.10E+04	2.44E+04	2.78E+04
U_o (W/m^2K)	5.03E+03	5.73E+03	6.55E+03	7.36E+03	8.03E+03	8.70E+03
UN (± %)	7.08E+00	6.19E+00	5.88E+00	5.75E+00	5.50E+00	5.37E+00

TABLE C.6: CONDENSATION OF HFC-236fa ON THE TURBO-CII TUBE AT A SATURATION TEMPERATURE OF 40°C (REPEAT RUN)

h (W/m^2K)	9.63E+03	1.04E+04	1.11E+04	1.24E+04	1.33E+04	1.43E+04
q'' (W/m^2)	1.53E+04	2.02E+04	2.49E+04	2.98E+04	3.49E+04	4.00E+04
q (Watts)	7.66E+02	1.01E+03	1.25E+03	1.50E+03	1.75E+03	2.01E+03
LMTD (°C)	3.10E+00	3.55E+00	3.93E+00	4.16E+00	4.46E+00	4.69E+00
ΔT (°C)	1.61E+00	1.82E+00	2.01E+00	2.12E+00	2.26E+00	2.38E+00
h_i (W/m^2K)	1.28E+04	1.62E+04	1.92E+04	2.21E+04	2.51E+04	2.78E+04
Re_i	1.07E+04	1.42E+04	1.75E+04	2.09E+04	2.44E+04	2.77E+04
U_o (W/m^2K)	5.00E+03	5.77E+03	6.45E+03	7.28E+03	7.96E+03	8.66E+03
UN (± %)	6.89E+00	6.32E+00	5.78E+00	5.64E+00	5.51E+00	5.39E+00

TABLE C.7: POOL BOILING OF HFC-236fa ON THE 1024-fpm TUBE AT A SATURATION TEMPERATURE OF 40°C (PRIMARY RUN)

h (W/m^2K)	7.55E+03	7.16E+03	6.64E+03	6.09E+03	5.42E+03	4.86E+03
q" (W/m^2)	3.99E+04	3.50E+04	3.00E+04	2.50E+04	1.99E+04	1.50E+04
q (Watts)	2.00E+03	1.76E+03	1.50E+03	1.25E+03	9.96E+02	7.53E+02
LMTD (°C)	1.08E+01	1.03E+01	9.79E+00	9.20E+00	8.53E+00	7.77E+00
Δ T (°C)	5.42E+00	5.17E+00	4.91E+00	4.62E+00	4.28E+00	3.91E+00
h_i (W/m^2K)	9.79E+03	8.74E+03	7.67E+03	6.60E+03	5.50E+03	4.31E+03
Re_i	1.78E+04	1.53E+04	1.30E+04	1.06E+04	8.41E+03	6.15E+03
U_o (W/m^2K)	3.69E+03	3.40E+03	3.06E+03	2.71E+03	2.33E+03	1.93E+03
UN (± %)	7.25E+00	7.53E+00	7.87E+00	8.30E+00	8.86E+00	9.81E+00

TABLE C.8: POOL BOILING OF HFC-236fa ON THE 1024-fpm TUBE AT A SATURATION TEMPERATURE OF 40°C (REPEAT RUN)

h (W/m^2K)	7.32E+03	7.02E+03	6.56E+03	6.03E+03	5.36E+03	4.78E+03
q" (W/m^2)	3.97E+04	3.49E+04	3.00E+04	2.50E+04	2.00E+04	1.50E+04
q (Watts)	1.99E+03	1.75E+03	1.50E+03	1.26E+03	1.01E+03	7.54E+02
LMTD (°C)	1.09E+01	1.04E+01	9.83E+00	9.28E+00	8.64E+00	7.83E+00
Δ T (°C)	5.47E+00	5.21E+00	4.93E+00	4.66E+00	4.34E+00	3.94E+00
h_i (W/m^2K)	9.79E+03	8.73E+03	7.69E+03	6.58E+03	5.50E+03	4.31E+03
Re_i	1.78E+04	1.53E+04	1.30E+04	1.06E+04	8.42E+03	6.16E+03
U_o (W/m^2K)	3.64E+03	3.36E+03	3.05E+03	2.70E+03	2.32E+03	1.92E+03
UN (± %)	7.15E+00	7.44E+00	7.80E+00	8.21E+00	8.72E+00	9.68E+00

TABLE C.9: POOL BOILING OF HFC-236fa ON THE 1575-fpm TUBE AT A SATURATION TEMPERATURE OF 40°C (PRIMARY RUN)

h (W/m^2K)	6.14E+03	5.81E+03	5.32E+03	4.80E+03	4.31E+03	3.74E+03
q'' (W/m^2)	3.99E+04	3.49E+04	3.00E+04	2.50E+04	1.99E+04	1.50E+04
q (Watts)	2.00E+03	1.75E+03	1.50E+03	1.25E+03	9.98E+02	7.51E+02
LMTD (°C)	1.19E+01	1.13E+01	1.08E+01	1.02E+01	9.39E+00	8.59E+00
ΔT (°C)	5.96E+00	5.67E+00	5.42E+00	5.12E+00	4.71E+00	4.32E+00
h_i (W/m^2K)	9.29E+03	8.28E+03	7.27E+03	6.24E+03	5.19E+03	4.05E+03
Re_i	1.68E+04	1.45E+04	1.22E+04	1.00E+04	7.91E+03	5.75E+03
U_o (W/m^2K)	3.38E+03	3.12E+03	2.80E+03	2.47E+03	2.14E+03	1.76E+03
UN (± %)	6.32E+00	6.54E+00	6.72E+00	6.97E+00	7.46E+00	8.02E+00

TABLE C.10: POOL BOILING OF HFC-236fa ON THE 1575-fpm TUBE AT A SATURATION TEMPERATURE OF 40°C (REPEAT RUN)

h (W/m^2K)	6.13E+03	5.75E+03	5.30E+03	4.84E+03	4.31E+03	3.66E+03
q'' (W/m^2)	3.99E+04	3.50E+04	3.00E+04	2.50E+04	1.98E+04	1.50E+04
q (Watts)	2.00E+03	1.75E+03	1.50E+03	1.25E+03	9.94E+02	7.52E+02
LMTD (°C)	1.19E+01	1.14E+01	1.08E+01	1.02E+01	9.36E+00	8.68E+00
ΔT (°C)	5.98E+00	5.71E+00	5.43E+00	5.10E+00	4.70E+00	4.36E+00
h_i (W/m^2K)	9.29E+03	8.27E+03	7.27E+03	6.24E+03	5.18E+03	4.07E+03
Re_i	1.68E+04	1.45E+04	1.22E+04	1.00E+04	7.88E+03	5.79E+03
U_o (W/m^2K)	3.38E+03	3.10E+03	2.80E+03	2.48E+03	2.14E+03	1.74E+03
UN (± %)	6.29E+00	6.48E+00	6.71E+00	7.02E+00	7.49E+00	7.90E+00

TABLE C.11: POOL BOILING OF HFC-236fa ON THE TURBO-B TUBE AT A SATURATION TEMPERATURE OF 40°C (PRIMARY RUN)

h (W/m^2K)	1.18E+04	1.16E+04	1.12E+04	1.04E+04	9.14E+03	7.97E+03
q'' (W/m^2)	3.98E+04	3.50E+04	3.00E+04	2.50E+04	2.00E+04	1.49E+04
q (Watts)	2.00E+03	1.76E+03	1.50E+03	1.26E+03	1.00E+03	7.48E+02
LMTD (°C)	5.88E+00	5.47E+00	5.03E+00	4.69E+00	4.33E+00	3.89E+00
ΔT (°C)	2.97E+00	2.76E+00	2.55E+00	2.38E+00	2.20E+00	1.98E+00
h_i (W/m^2K)	2.08E+04	1.86E+04	1.64E+04	1.40E+04	1.18E+04	9.26E+03
Re_i	1.38E+04	1.20E+04	1.01E+04	8.32E+03	6.64E+03	4.90E+03
U_o (W/m^2K)	6.97E+03	6.60E+03	6.14E+03	5.50E+03	4.75E+03	3.95E+03
UN (± %)	7.38E+00	7.93E+00	8.63E+00	9.26E+00	9.98E+00	1.12E+01

TABLE C.12: POOL BOILING OF HFC-236fa ON THE TURBO-B TUBE AT A SATURATION TEMPERATURE OF 40°C (REPEAT RUN)

h (W/m^2K)	1.18E+04	1.17E+04	1.11E+04	1.04E+04	9.09E+03	7.67E+03
q'' (W/m^2)	3.99E+04	3.50E+04	3.00E+04	2.50E+04	2.01E+04	1.51E+04
q (Watts)	2.00E+03	1.75E+03	1.50E+03	1.26E+03	1.01E+03	7.58E+02
LMTD (°C)	5.88E+00	5.44E+00	5.06E+00	4.69E+00	4.37E+00	4.02E+00
ΔT (°C)	2.97E+00	2.75E+00	2.56E+00	2.38E+00	2.22E+00	2.05E+00
h_i (W/m^2K)	2.08E+04	1.86E+04	1.63E+04	1.40E+04	1.17E+04	9.28E+03
Re_i	1.38E+04	1.19E+04	1.01E+04	8.34E+03	6.64E+03	4.92E+03
U_o (W/m^2K)	6.98E+03	6.62E+03	6.10E+03	5.50E+03	4.73E+03	3.88E+03
UN (± %)	7.38E+00	7.97E+00	8.56E+00	9.25E+00	9.89E+00	1.07E+01

TABLE C.13: POOL BOILING OF HFC-236fa ON THE TURBO-BII TUBE AT A SATURATION TEMPERATURE OF 40°C (PRIMARY RUN)

h (W/m^2K)	1.45E+04	1.45E+04	1.45E+04	1.46E+04	1.45E+04	1.39E+04
q'' (W/m^2)	4.00E+04	3.50E+04	3.00E+04	2.50E+04	2.00E+04	1.50E+04
q (Watts)	2.01E+03	1.76E+03	1.50E+03	1.26E+03	1.01E+03	7.55E+02
LMTD (°C)	5.61E+00	5.21E+00	4.77E+00	4.34E+00	3.89E+00	3.46E+00
ΔT (°C)	2.83E+00	2.64E+00	2.42E+00	2.21E+00	1.99E+00	1.78E+00
h_i (W/m^2K)	1.70E+04	1.52E+04	1.34E+04	1.15E+04	9.59E+03	7.58E+03
Re_i	1.37E+04	1.18E+04	1.00E+04	8.26E+03	6.55E+03	4.86E+03
U_o (W/m^2K)	7.10E+03	6.70E+03	6.25E+03	5.74E+03	5.12E+03	4.32E+03
UN (± %)	9.08E+00	9.99E+00	1.13E+01	1.31E+01	1.57E+01	1.94E+01

TABLE C.14: POOL BOILING OF HFC-236fa ON THE TURBO-BII TUBE AT A SATURATION TEMPERATURE OF 40°C (REPEAT RUN)

h (W/m^2K)	1.45E+04	1.45E+04	1.45E+04	1.47E+04	1.45E+04	1.39E+04
q'' (W/m^2)	4.00E+04	3.50E+04	3.00E+04	2.49E+04	2.00E+04	1.50E+04
q (Watts)	2.01E+03	1.76E+03	1.51E+03	1.25E+03	1.01E+03	7.55E+02
LMTD (°C)	5.61E+00	5.20E+00	4.79E+00	4.30E+00	3.90E+00	3.47E+00
ΔT (°C)	2.83E+00	2.63E+00	2.43E+00	2.19E+00	1.99E+00	1.78E+00
h_i (W/m^2K)	1.70E+04	1.52E+04	1.33E+04	1.15E+04	9.58E+03	7.55E+03
Re_i	1.37E+04	1.19E+04	1.00E+04	8.25E+03	6.55E+03	4.83E+03
U_o (W/m^2K)	7.11E+03	6.71E+03	6.25E+03	5.76E+03	5.12E+03	4.32E+03
UN (± %)	9.10E+00	1.00E+01	1.13E+01	1.33E+01	1.57E+01	1.94E+01

TABLE C.15: POOL BOILING OF HFC-236fa WITH 1% OIL ON THE 1024-fpm TUBE AT A SATURATION TEMPERATURE OF 40°C (PRIMARY RUN)

h (W/m^2K)	6.72E+03	6.43E+03	6.02E+03	5.57E+03	5.00E+03	4.28E+03
q'' (W/m^2)	3.99E+04	3.50E+04	3.00E+04	2.50E+04	2.00E+04	1.50E+04
q (Watts)	2.00E+03	1.76E+03	1.51E+03	1.25E+03	1.00E+03	7.55E+02
LMTD (°C)	1.14E+01	1.08E+01	1.02E+01	9.58E+00	8.87E+00	8.20E+00
ΔT (°C)	5.73E+00	5.43E+00	5.14E+00	4.81E+00	4.46E+00	4.12E+00
h_i (W/m^2K)	9.87E+03	8.81E+03	7.71E+03	6.62E+03	5.50E+03	4.32E+03
Re_i	1.81E+04	1.56E+04	1.31E+04	1.07E+04	8.45E+03	6.20E+03
U_o (W/m^2K)	3.49E+03	3.23E+03	2.93E+03	2.61E+03	2.25E+03	1.84E+03
UN (± %)	6.73E+00	7.03E+00	7.34E+00	7.78E+00	8.32E+00	8.89E+00

TABLE C.16: POOL BOILING OF HFC-236fa WITH 1% OIL ON THE 1024-fpm TUBE AT A SATURATION TEMPERATURE OF 40°C (REPEAT RUN)

h (W/m^2K)	6.76E+03	6.46E+03	6.03E+03	5.59E+03	5.06E+03	4.29E+03
q'' (W/m^2)	4.00E+04	3.50E+04	3.01E+04	2.50E+04	1.99E+04	1.50E+04
q (Watts)	2.01E+03	1.76E+03	1.51E+03	1.26E+03	1.00E+03	7.51E+02
LMTD (°C)	1.14E+01	1.08E+01	1.03E+01	9.58E+00	8.82E+00	8.15E+00
ΔT (°C)	5.72E+00	5.42E+00	5.15E+00	4.81E+00	4.43E+00	4.09E+00
h_i (W/m^2K)	9.86E+03	8.79E+03	7.71E+03	6.62E+03	5.50E+03	4.32E+03
Re_i	1.81E+04	1.55E+04	1.31E+04	1.07E+04	8.45E+03	6.19E+03
U_o (W/m^2K)	3.50E+03	3.24E+03	2.93E+03	2.61E+03	2.26E+03	1.84E+03
UN (± %)	6.75E+00	7.05E+00	7.33E+00	7.79E+00	8.38E+00	8.96E+00

TABLE C.17: POOL BOILING OF HFC-236fa WITH 1% OIL ON THE 1575-fpm TUBE AT A SATURATION TEMPERATURE OF 40°C (PRIMARY RUN)

h (W/m^2K)	5.92E+03	5.53E+03	5.09E+03	4.65E+03	4.38E+03	3.85E+03
q'' (W/m^2)	4.00E+04	3.49E+04	2.99E+04	2.50E+04	2.00E+04	1.50E+04
q (Watts)	2.01E+03	1.75E+03	1.50E+03	1.26E+03	1.00E+03	7.51E+02
LMTD (°C)	1.22E+01	1.16E+01	1.10E+01	1.04E+01	9.35E+00	8.49E+00
ΔT (°C)	6.10E+00	5.81E+00	5.53E+00	5.21E+00	4.69E+00	4.26E+00
h_i (W/m^2K)	9.30E+03	8.29E+03	7.30E+03	6.24E+03	5.20E+03	4.05E+03
Re_i	1.69E+04	1.45E+04	1.23E+04	1.01E+04	7.91E+03	5.73E+03
U_o (W/m^2K)	3.32E+03	3.04E+03	2.74E+03	2.43E+03	2.16E+03	1.78E+03
UN (± %)	6.15E+00	6.35E+00	6.56E+00	6.82E+00	7.51E+00	8.18E+00

TABLE C.18: POOL BOILING OF HFC-236fa WITH 1% OIL ON THE 1575-fpm TUBE AT A SATURATION TEMPERATURE OF 40°C (REPEAT RUN)

h (W/m^2K)	5.91E+03	5.51E+03	5.08E+03	4.65E+03	4.24E+03	3.68E+03
q'' (W/m^2)	4.01E+04	3.49E+04	2.99E+04	2.50E+04	2.01E+04	1.51E+04
q (Watts)	2.01E+03	1.75E+03	1.50E+03	1.26E+03	1.01E+03	7.56E+02
LMTD (°C)	1.22E+01	1.16E+01	1.10E+01	1.04E+01	9.57E+00	8.71E+00
ΔT (°C)	6.11E+00	5.81E+00	5.53E+00	5.21E+00	4.80E+00	4.37E+00
h_i (W/m^2K)	9.31E+03	8.31E+03	7.29E+03	6.26E+03	5.19E+03	4.06E+03
Re_i	1.69E+04	1.46E+04	1.23E+04	1.01E+04	7.92E+03	5.76E+03
U_o (W/m^2K)	3.32E+03	3.03E+03	2.74E+03	2.43E+03	2.12E+03	1.75E+03
UN (± %)	6.14E+00	6.34E+00	6.56E+00	6.83E+00	7.29E+00	7.88E+00

TABLE C.19: POOL BOILING OF HFC-236fa WITH 1% OIL ON THE TURBO-B TUBE AT A SATURATION TEMPERATURE OF 40°C (PRIMARY RUN)

h (W/m^2K)	1.32E+04	1.26E+04	1.19E+04	1.10E+04	9.98E+03	8.60E+03
q'' (W/m^2)	4.00E+04	3.50E+04	2.99E+04	2.49E+04	2.00E+04	1.50E+04
q (Watts)	2.01E+03	1.75E+03	1.50E+03	1.25E+03	1.00E+03	7.55E+02
LMTD (°C)	5.56E+00	5.23E+00	4.87E+00	4.53E+00	4.15E+00	3.78E+00
ΔT (°C)	2.81E+00	2.65E+00	2.47E+00	2.30E+00	2.11E+00	1.93E+00
h_i (W/m^2K)	2.07E+04	1.85E+04	1.63E+04	1.40E+04	1.17E+04	9.25E+03
Re_i	1.37E+04	1.19E+04	1.00E+04	8.30E+03	6.60E+03	4.89E+03
U_o (W/m^2K)	7.41E+03	6.89E+03	6.33E+03	5.66E+03	4.96E+03	4.10E+03
UN (± %)	7.93E+00	8.42E+00	9.05E+00	9.73E+00	1.07E+01	1.19E+01

TABLE C.20: POOL BOILING OF HFC-236fa WITH 1% OIL ON THE TURBO-B TUBE AT A SATURATION TEMPERATURE OF 40°C (REPEAT RUN)

h (W/m^2K)	1.31E+04	1.26E+04	1.19E+04	1.10E+04	9.96E+03	8.65E+03
q'' (W/m^2)	4.00E+04	3.50E+04	3.00E+04	2.50E+04	2.00E+04	1.50E+04
q (Watts)	2.01E+03	1.76E+03	1.51E+03	1.26E+03	1.00E+03	7.50E+02
LMTD (°C)	5.56E+00	5.23E+00	4.89E+00	4.56E+00	4.15E+00	3.76E+00
ΔT (°C)	2.81E+00	2.65E+00	2.48E+00	2.31E+00	2.12E+00	1.92E+00
h_i (W/m^2K)	2.07E+04	1.85E+04	1.63E+04	1.40E+04	1.17E+04	9.21E+03
Re_i	1.37E+04	1.18E+04	1.00E+04	8.33E+03	6.61E+03	4.86E+03
U_o (W/m^2K)	7.41E+03	6.90E+03	6.33E+03	5.66E+03	4.95E+03	4.10E+03
UN (± %)	7.93E+00	8.42E+00	9.01E+00	9.67E+00	1.07E+01	1.20E+01

TABLE C.21: POOL BOILING OF HFC-236fa WITH 1% OIL ON THE TURBO-BII TUBE AT A SATURATION TEMPERATURE OF 40°C (PRIMARY RUN)

h (W/m^2K)	1.90E+04	1.90E+04	1.88E+04	1.85E+04	1.77E+04	1.55E+04
q" (W/m^2)	3.99E+04	3.50E+04	3.00E+04	2.51E+04	2.01E+04	1.52E+04
q (Watts)	2.00E+03	1.76E+03	1.50E+03	1.26E+03	1.01E+03	7.61E+02
LMTD (°C)	4.96E+00	4.65E+00	4.32E+00	4.00E+00	3.65E+00	3.38E+00
Δ T (°C)	2.51E+00	2.36E+00	2.20E+00	2.04E+00	1.87E+00	1.74E+00
h_i (W/m^2K)	1.69E+04	1.51E+04	1.33E+04	1.14E+04	9.56E+03	7.56E+03
Re_i	1.35E+04	1.16E+04	9.91E+03	8.19E+03	6.52E+03	4.84E+03
U_o (W/m^2K)	8.01E+03	7.48E+03	6.91E+03	6.25E+03	5.47E+03	4.47E+03
UN (± %)	1.13E+01	1.25E+01	1.41E+01	1.61E+01	1.88E+01	2.13E+01

TABLE C.22: POOL BOILING OF HFC-236fa WITH 1% OIL ON THE TURBO-BII TUBE AT A SATURATION TEMPERATURE OF 40°C (REPEAT RUN)

h (W/m^2K)	1.93E+04	1.92E+04	1.92E+04	1.88E+04	1.80E+04	1.56E+04
q" (W/m^2)	4.00E+04	3.49E+04	3.00E+04	2.51E+04	2.00E+04	1.51E+04
q (Watts)	2.01E+03	1.75E+03	1.50E+03	1.26E+03	1.00E+03	7.60E+02
LMTD (°C)	4.94E+00	4.62E+00	4.29E+00	3.98E+00	3.62E+00	3.37E+00
Δ T (°C)	2.50E+00	2.35E+00	2.18E+00	2.03E+00	1.85E+00	1.73E+00
h_i (W/m^2K)	1.69E+04	1.51E+04	1.33E+04	1.14E+04	9.57E+03	7.57E+03
Re_i	1.35E+04	1.16E+04	9.90E+03	8.17E+03	6.52E+03	4.85E+03
U_o (W/m^2K)	8.06E+03	7.53E+03	6.97E+03	6.28E+03	5.50E+03	4.48E+03
UN (± %)	1.15E+01	1.27E+01	1.43E+01	1.63E+01	1.92E+01	2.15E+01

TABLE C.23: POOL BOILING OF HFC-236fa WITH 3% OIL ON THE 1024-fpm TUBE AT A SATURATION TEMPERATURE OF 40°C (PRIMARY RUN)

h (W/m^2K)	6.87E+03	6.49E+03	6.09E+03	5.58E+03	5.06E+03	4.34E+03
q'' (W/m^2)	4.00E+04	3.50E+04	3.00E+04	2.50E+04	2.01E+04	1.50E+04
q (Watts)	2.00E+03	1.76E+03	1.50E+03	1.25E+03	1.01E+03	7.55E+02
LMTD (°C)	1.13E+01	1.08E+01	1.02E+01	9.58E+00	8.88E+00	8.15E+00
ΔT (°C)	5.68E+00	5.41E+00	5.11E+00	4.81E+00	4.46E+00	4.09E+00
h_i (W/m^2K)	9.85E+03	8.79E+03	7.72E+03	6.61E+03	5.50E+03	4.32E+03
Re_i	1.80E+04	1.55E+04	1.31E+04	1.07E+04	8.46E+03	6.19E+03
U_o (W/m^2K)	3.53E+03	3.25E+03	2.95E+03	2.61E+03	2.26E+03	1.85E+03
UN (± %)	6.81E+00	7.07E+00	7.40E+00	7.78E+00	8.33E+00	9.00E+00

TABLE C.24: POOL BOILING OF HFC-236fa WITH 3% OIL ON THE 1024-fpm TUBE AT A SATURATION TEMPERATURE OF 40°C (REPEAT RUN)

h (W/m^2K)	6.89E+03	6.54E+03	6.11E+03	5.61E+03	5.08E+03	4.36E+03
q'' (W/m^2)	4.00E+04	3.50E+04	3.00E+04	2.51E+04	2.00E+04	1.51E+04
q (Watts)	2.01E+03	1.76E+03	1.51E+03	1.26E+03	1.01E+03	7.55E+02
LMTD (°C)	1.13E+01	1.07E+01	1.02E+01	9.60E+00	8.84E+00	8.14E+00
ΔT (°C)	5.67E+00	5.38E+00	5.10E+00	4.82E+00	4.44E+00	4.09E+00
h_i (W/m^2K)	9.84E+03	8.79E+03	7.70E+03	6.61E+03	5.50E+03	4.32E+03
Re_i	1.80E+04	1.55E+04	1.31E+04	1.07E+04	8.46E+03	6.20E+03
U_o (W/m^2K)	3.53E+03	3.26E+03	2.95E+03	2.62E+03	2.27E+03	1.85E+03
UN (± %)	6.82E+00	7.11E+00	7.42E+00	7.77E+00	8.38E+00	9.01E+00

TABLE C.25: POOL BOILING OF HFC-236fa WITH 3% OIL ON THE 1575-fpm TUBE AT A SATURATION TEMPERATURE OF 40°C (PRIMARY RUN)

h (W/m^2K)	6.14E+03	5.74E+03	5.32E+03	4.91E+03	4.41E+03	3.83E+03
q'' (W/m^2)	4.01E+04	3.50E+04	2.96E+04	2.50E+04	2.00E+04	1.49E+04
q (Watts)	2.01E+03	1.76E+03	1.48E+03	1.26E+03	1.01E+03	7.50E+02
LMTD (°C)	1.20E+01	1.14E+01	1.07E+01	1.01E+01	9.37E+00	8.49E+00
ΔT (°C)	6.00E+00	5.72E+00	5.35E+00	5.07E+00	4.70E+00	4.26E+00
h_i (W/m^2K)	9.29E+03	8.29E+03	7.25E+03	6.22E+03	5.17E+03	4.05E+03
Re_i	1.68E+04	1.45E+04	1.22E+04	9.99E+03	7.87E+03	5.74E+03
U_o (W/m^2K)	3.38E+03	3.10E+03	2.80E+03	2.50E+03	2.16E+03	1.78E+03
UN (± %)	6.27E+00	6.46E+00	6.81E+00	7.07E+00	7.50E+00	8.16E+00

TABLE C.26: POOL BOILING OF HFC-236fa WITH 3% OIL ON THE 1575-fpm TUBE AT A SATURATION TEMPERATURE OF 40°C (REPEAT RUN)

h (W/m^2K)	6.31E+03	5.94E+03	5.46E+03	4.96E+03	4.45E+03	3.86E+03
q'' (W/m^2)	4.00E+04	3.50E+04	3.00E+04	2.50E+04	2.00E+04	1.50E+04
q (Watts)	2.01E+03	1.75E+03	1.50E+03	1.25E+03	1.01E+03	7.55E+02
LMTD (°C)	1.18E+01	1.12E+01	1.07E+01	1.00E+01	9.34E+00	8.50E+00
ΔT (°C)	5.91E+00	5.61E+00	5.35E+00	5.04E+00	4.69E+00	4.27E+00
h_i (W/m^2K)	9.24E+03	8.26E+03	7.25E+03	6.22E+03	5.17E+03	4.06E+03
Re_i	1.67E+04	1.44E+04	1.22E+04	9.98E+03	7.86E+03	5.75E+03
U_o (W/m^2K)	3.43E+03	3.15E+03	2.84E+03	2.51E+03	2.17E+03	1.79E+03
UN (± %)	6.37E+00	6.62E+00	6.84E+00	7.13E+00	7.54E+00	8.16E+00

TABLE C.27: POOL BOILING OF HFC-236fa WITH 3% OIL ON THE TURBO-B TUBE AT A SATURATION TEMPERATURE OF 40°C (PRIMARY RUN)

h (W/m^2K)	1.25E+04	1.21E+04	1.14E+04	1.04E+04	9.36E+03	8.23E+03
q" (W/m^2)	4.00E+04	3.50E+04	3.00E+04	2.50E+04	2.00E+04	1.50E+04
q (Watts)	2.00E+03	1.76E+03	1.51E+03	1.26E+03	1.00E+03	7.54E+02
LMTD (°C)	5.73E+00	5.34E+00	5.00E+00	4.69E+00	4.29E+00	3.86E+00
Δ T (°C)	2.89E+00	2.70E+00	2.53E+00	2.38E+00	2.19E+00	1.97E+00
h_i (W/m^2K)	2.07E+04	1.86E+04	1.63E+04	1.40E+04	1.17E+04	9.23E+03
Re_i	1.37E+04	1.19E+04	1.01E+04	8.32E+03	6.64E+03	4.88E+03
U_o (W/m^2K)	7.19E+03	6.75E+03	6.18E+03	5.50E+03	4.80E+03	4.01E+03
UN (± %)	7.63E+00	8.17E+00	8.70E+00	9.25E+00	1.01E+01	1.15E+01

TABLE C.28: POOL BOILING OF HFC-236fa WITH 3% OIL ON THE TURBO-B TUBE AT A SATURATION TEMPERATURE OF 40°C (REPEAT RUN)

h (W/m^2K)	1.25E+04	1.20E+04	1.13E+04	1.03E+04	9.36E+03	8.17E+03
q" (W/m^2)	4.00E+04	3.50E+04	3.00E+04	2.50E+04	2.00E+04	1.50E+04
q (Watts)	2.01E+03	1.76E+03	1.51E+03	1.26E+03	1.00E+03	7.54E+02
LMTD (°C)	5.73E+00	5.37E+00	5.03E+00	4.70E+00	4.29E+00	3.88E+00
Δ T (°C)	2.89E+00	2.72E+00	2.55E+00	2.38E+00	2.18E+00	1.98E+00
h_i (W/m^2K)	2.07E+04	1.86E+04	1.63E+04	1.40E+04	1.17E+04	9.23E+03
Re_i	1.37E+04	1.19E+04	1.01E+04	8.32E+03	6.62E+03	4.89E+03
U_o (W/m^2K)	7.19E+03	6.72E+03	6.14E+03	5.49E+03	4.80E+03	3.99E+03
UN (± %)	7.64E+00	8.11E+00	8.63E+00	9.23E+00	1.02E+01	1.14E+01

TABLE C.29: POOL BOILING OF HFC-236fa WITH 3% OIL ON THE TURBO-BII TUBE AT A SATURATION TEMPERATURE OF 40°C (PRIMARY RUN)

h (W/m^2K)	1.68E+04	1.66E+04	1.62E+04	1.54E+04	1.42E+04	1.22E+04
q" (W/m^2)	3.99E+04	3.50E+04	3.00E+04	2.50E+04	2.00E+04	1.50E+04
q (Watts)	2.00E+03	1.76E+03	1.51E+03	1.26E+03	1.00E+03	7.53E+02
LMTD (°C)	5.23E+00	4.91E+00	4.57E+00	4.26E+00	3.91E+00	3.61E+00
Δ T (°C)	2.65E+00	2.49E+00	2.32E+00	2.17E+00	2.00E+00	1.85E+00
h_i (W/m^2K)	1.69E+04	1.51E+04	1.33E+04	1.14E+04	9.58E+03	7.56E+03
Re_i	1.36E+04	1.17E+04	9.98E+03	8.22E+03	6.55E+03	4.85E+03
U_o (W/m^2K)	7.59E+03	7.11E+03	6.54E+03	5.86E+03	5.09E+03	4.15E+03
UN (± %)	1.02E+01	1.12E+01	1.24E+01	1.37E+01	1.55E+01	1.73E+01

TABLE C.30: POOL BOILING OF HFC-236fa WITH 3% OIL ON THE TURBO-BII TUBE AT A SATURATION TEMPERATURE OF 40°C (REPEAT RUN)

h (W/m^2K)	1.68E+04	1.65E+04	1.61E+04	1.53E+04	1.39E+04	1.18E+04
q" (W/m^2)	4.00E+04	3.50E+04	3.00E+04	2.51E+04	2.00E+04	1.50E+04
q (Watts)	2.01E+03	1.76E+03	1.51E+03	1.26E+03	1.01E+03	7.55E+02
LMTD (°C)	5.25E+00	4.92E+00	4.58E+00	4.28E+00	3.95E+00	3.66E+00
Δ T (°C)	2.66E+00	2.49E+00	2.33E+00	2.18E+00	2.02E+00	1.87E+00
h_i (W/m^2K)	1.69E+04	1.51E+04	1.33E+04	1.15E+04	9.58E+03	7.56E+03
Re_i	1.36E+04	1.17E+04	9.98E+03	8.22E+03	6.55E+03	4.85E+03
U_o (W/m^2K)	7.60E+03	7.09E+03	6.53E+03	5.84E+03	5.05E+03	4.09E+03
UN (± %)	1.02E+01	1.11E+01	1.23E+01	1.36E+01	1.51E+01	1.67E+01

APPENDIX D

DERIVATION OF UNCERTAINTY ANALYSIS EQUATIONS

This appendix presents the derivation of uncertainty analysis equations for the shell-side heat transfer coefficients calculated in this study.

Substituting q and LMTD in Equation 4.4 by those given in Equations 4.2 and 4.3 and replacing U_o and R_w in Equation 4.5 by those given in the Equation 4.4 and Equation 4.6 results in the following equation for the shell-side heat transfer coefficient (h),

$$h = \left[\frac{A_o}{\dot{m}_i \cdot Cp_i \cdot \ln\left(\frac{T_{sat} - T_{i,in}}{T_{sat} - T_{i,out}}\right)} - \frac{A_o}{A_i}\frac{1}{h_i} - \frac{A_o \ln(D_o/D_i)}{2\pi k_w L} \right]^{-1} \tag{D.1}$$

Equation D.1 shows that for a given heat exchanger (tube) the uncertainty of h depends on the seven variables: $\dot{m}_i$, Cp_i, h_i, k_w, T_{sat}, $T_{i,out}$, and $T_{i,in}$. The other terms in Equation D.1 are constants for a given tube since D_o and D_i (and thus A_o and A_i) are constants. Therefore, the uncertainty in the calculated shell-side heat transfer coefficient according to the propagation of error approach described in the Phase I report [13] is defined as

$$\delta h = \left[\left(\frac{\partial h}{\partial \dot{m}_i}(\delta \dot{m}_i)\right)^2 + \left(\frac{\partial h}{\partial Cp_i}(\delta Cp_i)\right)^2 + \left(\frac{\partial h}{\partial h_i}(\delta h_i)\right)^2 + \left(\frac{\partial h}{\partial k_w}(\delta k_w)\right)^2 + \left(\frac{\partial h}{\partial T_{sat}}(\delta T_{sat})\right)^2 + \left(\frac{\partial h}{\partial T_{i,out}}(\delta T_{i,out})\right)^2 + \left(\frac{\partial h}{\partial T_{i,in}}(\delta T_{i,in})\right)^2 \right]^{1/2} \tag{D.2}$$

where $\delta \dot{m}_i$ is the uncertainty of the water mass flow rate, δCp_i is the uncertainty of the water's specific heat, δh_i is the uncertainty of the in-tube heat transfer coefficient, and δk_w is the uncertainty of the thermal conductivity of tube wall (k_w, W/m·K). δk_w was calculated using the tube wall temperature ($T_w = (T_{sat}+T_{i,bulk})/2$, °C) while δCp_i

was calculated based on the bulk water temperature ($T_{i,bulk}$ =($T_{i,in}$+ $T_{i,out}$)/2). The remaining three terms (δT_{sat}, $\delta T_{i,out}$, and $\delta T_{i,in}$) are referred to the uncertainty due to the temperature measurements of the refrigerant saturation temperature, and the water outlet and water inlet temperatures, respectively. The uncertainty in the shell-side heat transfer coefficient was caused by the existing uncertainty in the measurements. The instrumentation accuracy of the test facility is summarized in Chapter 4.

The following equations which are the partial derivatives of Equation D.1 with respect to the six independent variables are required in the determination of the uncertainty in the calculated shell-side heat transfer coefficients (i.e., Equation D.2).

$$\frac{\partial h}{\partial \dot{m}_i} = -h^2 \cdot \frac{-A_o}{\dot{m}_i^{\,2} \cdot Cp_i \cdot \ln\left(\frac{T_{sat} - T_{i,in}}{T_{sat} - T_{i,out}}\right)} \tag{D.3}$$

$$\frac{\partial h}{\partial Cp_i} = -h^2 \cdot \frac{-A_o}{\dot{m}_i \cdot Cp_i^{\,2} \cdot \ln\left(\frac{T_{sat} - T_{i,in}}{T_{sat} - T_{i,out}}\right)} \tag{D.4}$$

$$\frac{\partial h}{\partial h_i} = h^2 \cdot \left(\frac{A_o}{A_i}\frac{1}{h_i^{\,2}}\right) \tag{D.5}$$

$$\frac{\partial h}{\partial k_w} = -h^2 \cdot \frac{A_o \ln(D_o / D_i)}{2\pi k_w^{\,2} L} \tag{D.6}$$

$$\frac{\partial h}{\partial T_{sat}} = -h^2 \cdot \frac{A_o}{\dot{m}_i \cdot Cp_i} \cdot \frac{-1}{\left[\ln\left(\frac{T_{sat} - T_{i,in}}{T_{sat} - T_{i,out}}\right)\right]^2} \cdot \left(\frac{1}{T_{sat} - T_{i,in}} - \frac{1}{T_{sat} - T_{i,out}}\right) \tag{D.7}$$

For the calculation of the uncertainty in condensation,

$$\frac{\partial h}{\partial T_{i,out}} = -h^2 \cdot \frac{A_o}{\dot{m}_i \cdot Cp_i} \cdot \frac{-1}{\left[\ln\left(\frac{T_{sat} - T_{i,in}}{T_{sat} - T_{i,out}}\right)\right]^2} \cdot \left(\frac{1}{T_{sat} - T_{i,out}}\right) \tag{D.8}$$

$$\frac{\partial h}{\partial T_{i,in}} = -h^2 \cdot \frac{A_o}{\dot{m}_i \cdot Cp_i} \cdot \frac{-1}{\left[\ln\left(\frac{T_{sat} - T_{i,in}}{T_{sat} - T_{i,out}}\right)\right]^2} \cdot \left(\frac{-1}{T_{sat} - T_{i,in}}\right) \qquad (D.9)$$

While for the calculation of the uncertainty in evaporation, Equation D.1 becomes

$$h = \left[\frac{A_o}{\dot{m}_i \cdot Cp_i \cdot \ln\left(\frac{T_{i,in} - T_{sat}}{T_{i,out} - T_{sat}}\right)} - \frac{A_o}{A_i}\frac{1}{h_i} - \frac{A_o \ln(D_o/D_i)}{2\pi k_w L}\right]^{-1} \qquad (D.10)$$

The partial derivatives of Equation D.10 with respect to the seven independent variables are the same as those of Equation D.1; i.e., Equations D.3 through D.9 can also be used to determine the uncertainty in evaporation.

The estimate of uncertainty is listed in Tables 4.1 and 4.2 and Appendix C and is presented as a percentage of the calculated heat transfer coefficient; i.e., $(\delta h/h)\times 100$.

TECHNICAL REPORT DATA (Please read Instructions on the reverse before completing)		
1. REPORT NO. EPA-600/R-98-029	2.	3. RECIPIENT'S ACCESSION NO.
4. TITLE AND SUBTITLE Heat Transfer Evaluation of HFC-236fa in Condensation and Evaporation		5. REPORT DATE March 1998 6. PERFORMING ORGANIZATION CODE
7. AUTHOR(S) S.-M. Tzuoo and M. B. Pate		8. PERFORMING ORGANIZATION REPORT NO.
9. PERFORMING ORGANIZATION NAME AND ADDRESS Iowa State University Department of Mechanical Engineering Ames, Iowa 50011		10. PROGRAM ELEMENT NO. 11. CONTRACT/GRANT NO. EPA Purchase Order 5D2520NAEX
12. SPONSORING AGENCY NAME AND ADDRESS EPA, Office of Research and Development Air Pollution Prevention and Control Division Research Triangle Park, NC 27711		13. TYPE OF REPORT AND PERIOD COVERED Task Final; 9/95 - 5/96 14. SPONSORING AGENCY CODE EPA/600/13

15. SUPPLEMENTARY NOTES APPCD project officer is Theodore G. Brna, Mail Drop 4, 919/541-2683.

16. ABSTRACT The report gives results of an evaluation of the shell-side heat transfer performance of hydrofluorocarbon (HFC)-236fa, which is considered to be a potential substitute for chlorofluorocarbon (CFC)-114 in Navy shipboard chillers, for both conventional finned (1024- and 1575-fpm--fins-per-meter) tubes and high performance enhanced (Turbo-CII, -B, and -BII) tubes. Condensation of oil-free HFC-236fa was conducted on 1024- and -1575-fpm, and Turbo-CII tubes. Pool boiling on four tube types (1024- and 1575-fpm, and Turbo-B and -BII) was tested not only for pure HFC-236fa but also for HFC-236fa mixed with 1 and 3% lubricant by weight. The polyol-ester lubricant used has a viscosity of 340 SSU at 37.8 C (100 F) and the trade name of Castrol Icematic SW-68. The above tubes, which have nominal outside diameters of 19.1 mm (3/4-in.), were evaluated at a saturation temperature of 40 C for condensation and 2 C for pool boiling over the heat flux range of 15 to 40 kW/sq m. Heat transfer was improved for HFC-236fa by using the high performance enhanced tubes. Specifically, the Turbo-CII tube performed better than the two conventional finned tubes in the condensation testing, while the performance of the Turbo-B and -BII tubes was superior to the two conventional finned tubes in the pool boiling testing.

17. KEY WORDS AND DOCUMENT ANALYSIS		
a. DESCRIPTORS	b. IDENTIFIERS/OPEN ENDED TERMS	c. COSATI Field/Group
Pollution Coolers Heat Transfer Refrigerants	Pollution Prevention Stationary Sources Chillers Shipboard Equipment	13B 13A 20M
18. DISTRIBUTION STATEMENT Release to Public	19. SECURITY CLASS (This Report) Unclassified 20. SECURITY CLASS (This page) Unclassified	21. NO. OF PAGES 73 22. PRICE

EPA Form 2220-1 (9-73)